AROMATICS OXIDATION AND SOOT FORMATION IN FLAMES

J. B. Howard and H. Richter
MIT Department of Chemical Engineering
77 Massachusetts Avenue
Cambridge, MA 02139-4307
e-mail: jbhoward@mit.edu

Personnel involved:

Prof. Jack B. Howard, PI. Department of Chemical Engineering, MIT
Dr. Henning Richter, Research Associate, Department of Chemical Engineering, MIT
Murray J. Height, Graduate Student, Department of Chemical Engineering, MIT
Timothy G. Benish, Graduate Student, Department of Chemical Engineering, MIT
Dr. Peter Hebgen, Postdoctoral Associate, Department of Chemical Engineering, MIT
Dr. Arthur L. Lafleur, Associate Director, Center of Environmental Health Sciences, MIT
Dr. Koli Taghizadeh, Research Scientist, Center of Environmental Health Sciences, MIT
Dr. Atena Necula, Postdoctoral Associate, Department of Chemistry, Boston College
Prof. Lawrence T. Scott, Department of Chemistry, Boston College

Scope

This project is concerned with the kinetics and mechanisms of aromatics oxidation and the growth process to polycyclic aromatic hydrocarbons (PAH) of increasing size, soot and fullerenes formation in flames. The overall objective of the experimental aromatics oxidation work is to extend the set of available data by measuring concentration profiles for decomposition intermediates such as phenyl, cyclopentadienyl, phenoxy or indenyl radicals which could not be measured with molecular-beam mass spectrometry to permit further refinement and testing of benzene oxidation mechanisms. The focus includes PAH radicals which are thought to play a major role in the soot formation process while their concentrations are in many cases too low to permit measurement with conventional mass spectrometry. The radical species measurements are used in critical testing and improvement of a kinetic model describing benzene oxidation and PAH growth. Thermodynamic property data of selected species are determined computationally, for instance using density functional theory (DFT). Potential energy surfaces are explored in order to identify additional reaction pathways. The ultimate goal is to understand the conversion of high molecular weight compounds to nascent soot particles, to assess the roles of planar and curved PAH and relationships between soot and fullerenes formation. The specific aims are to characterize both the high molecular weight compounds involved in the nucleation of soot particles and the structure of soot including internal nanoscale features indicative of contributions of planar and/or curved PAH to particle inception.

Recent Progress

A) Experimental

Experimental work assessing PAH reaction pathways has been finished. Mole fraction profiles of PAH radicals and the corresponding parent molecules were determined using nozzle beam sampling followed by radical scavenging reactions with dimethyl disulfide. Scavening products, i.e., methylthio compounds (R-SCH_3) and stable PAH were analysed by gas chromatography

coupled with mass spectrometry (GC-MS). PAH isomers including specific radical sites were unambiguously identified using authentic standards, commercially available or synthesized in the present work. Two benzene/oxygen/argon flames (30% argon, cold gas velocity v= 50 cm s^{-1}, 20 torr) which were nearly sooting or slightly sooting with equivalence ratios of ϕ= 1.8 and 2.0, respectively, were investigated. All PAH profiles in the ϕ= 2.0 flame were shifted by ≈ 2 mm towards the burned gases compared to the ϕ= 1.8 flame. No increase of peak mole fractions was observed for one- and two-ring aromatics while an at least 2-fold increase was found for larger PAH. Experimental uncertainties were assessed by means of control experiments using equipment developed and built by Homann and coworkers, including combustion chamber, sampling and scavenging equipment. Shape and location of all measured compounds were very similar in both experiments while peak mole fractions were mostly lower in the control experiments. The results of the comparison ranged from a nearly perfect match such as for indene to ≈ 2 – 5-fold discrepancies. Larger discrepancies, observed in a few cases such as for 5-ethynylacenaphthylene, were attributed to possible experimental errors, e.g., incomplete peak separation in the GC analysis. As a general trend, partial equilibrium of (8) PAH + H ⇆ PAH• + H_2 is more and more closely approached with increasing size of the molecule. The experimental 2-naphthyl : phenyl mole fraction ratio was found to exceed the partial equilibrium value. Therefore, decomposition of PAH radicals forming butadiyne, e.g., the reverse of reaction (10) phenyl + C_4H_2 ⇆ 2-naphthyl is suggested as contributing to the consumption of some PAH radicals. Thermodynamic considerations were found to be important but not sufficient for a complete understanding of PAH formation and consumption. Background, data, their analysis and conclusion are reported below.

Introduction

Improved prevention of combustion-generated pollution requires better understanding of both the formation and destruction of pollutants and their precursors in flames. There is increasing evidence that polycyclic aromatic hydrocarbons (PAH) are key intermediates in the inception and growth of soot which is a major fraction of atmospheric aerosols [1,2]. The hazardous health effects of atmospheric aerosols [3-5] might partially be related to their association with PAH [6], some of which are mutagenic [7]. Fuel-rich combustion is also of significant interest in material synthesis. For instance, it is a well-established process for carbon black production [8] and is suitable for synthesis of fullerenes [9-14] and carbon nanostructures such as nanotubes [15-20].

The qualitative and quantitative understanding of combustion processes in general and of the growth of PAH, soot and fullerenic structures in particular, requires experimental and theoretical approaches. The availability of reliable experimental concentrations of reactants, intermediates and products in well-defined experimental setups such as well-stirred or plug-flow reactors [21-26], premixed flames [27-50] and shock tubes [51-57] is essential for meaningful assessment of chemical reaction pathways responsible for the combustion process by means of detailed kinetic networks. For instance, concentration profiles for stable species including PAH were measured in premixed low-pressure and atmospheric-pressure flames using a large range of aliphathic and aromatic fuels such as methane [27-29], ethane [29], ethylene [30-34], acetylene [30,35-38], propene [36,39], propane [37], 1,3-butadiene [40], cyclopentene [41], benzene [42-49] and naphthalene [50]. Modeling using detailed reaction networks has been used for the description of the formation of PAH of increasing size and has greatly contributed to the understanding of fuel-rich combustion over the last two decades [24,29,33,34,54,58-63]. Detailed modeling of soot formation has been attempted with some success using reaction schemes consisting of PAH

growth, soot-particle inception, surface growth, coagulation and soot oxidation [63-69]. Nevertheless, significant uncertainties persist in the quantitative understanding of PAH and soot oxidation [70], the relative contribution of acetylene and PAH to surface growth [31,71-72] and particularly, the details of particle inception. Experimental data of species in the mass range covering nascent soot particles are difficult to obtain and therefore very scarce. No definitive description of the transition from PAH to soot has been achieved and quantitative assessment of the competition between reaction pathways leading to soot and fullerenic material still needs to be addressed [73]. Also, the contribution of polyacetylenes to soot formation [1,2] has not been entirely ruled out [74]. The combination of different experimental techniques such as molecular beam sampling coupled to mass spectrometry (MBMS) [35,36,38-42,45,49], probe sampling with subsequent chromatographic analysis [21,24-27,29-33,37,44,47,48], optical techniques [28,32,36,38,39,46] and electron microscopy [18] provide valuable information concerning the main pathways of particle growth in fuel-rich hydrocarbon combustion. However, these techniques are of limited or no use for the determination of PAH radicals, which are expected to play a key role in the growth of molecules of increasing size. In most of the reaction schemes considered for PAH growth, such as the largely used hydrogen-abstraction/acetylene-addition mechanism [64], formation of radicals via hydrogen abstraction from the parent molecules is thought to be the initial activation step followed by reaction with, e.g., acetylene or other PAH. The position of the radical site determines the direction of the growth process while the number of possible sites increases with molecule size. MBMS allowed for the determination of concentration profiles of some PAH radicals [42], but, due to the similarity of their ionization potentials, only concentration profiles of sums of the different isomers could be measured.

Finally, significant progress was achieved by Homann and coworkers [43,50,75-77] with the development and use of a radical scavenging technique, consisting of nozzle beam sampling followed by reaction with the radical scavenger dimethyl disulfide (DMDS). This technique combines the freezing of the flame gas composition by molecular beam-type sampling with rapid stabilization of radicals by the scavenger, which is injected into the sample stream. The resulting scavenging products, together with stable compounds present in the sampled gases were then analyzed by chromatographic techniques. This method has been successfully applied to premixed low-pressure methane [77], acetylene [43,76,77], ethylene [77], 1-3-butadiene [77], benzene [43] and naphthalene [50] flames. A large range of species including stable PAH containing up to seven condensed aromatic rings and PAH radicals with one and two aromatic rings, i.e., indenyl, 1- and 2-naphthyl were unambiguously identified and the corresponding concentration profiles measured [50].

In the present work, an experimental setup previously used for the investigation of low-pressure premixed flat flames by means of MBMS [40,42,78] was modified for the use of nozzle-beam sampling coupled to radical scavenging by DMDS [79]. Radical scavenging by DMDS was used for the investigation of two nearly sooting [42] and sooting [42,44] low-pressure benzene/oxygen/argon flames, previously studied by means of MBMS [42] and, in the latter case also by probe sampling with subsequent chromatographic analysis [44,81]. These two conditions were selected in order to assess changes in the flame structure occurring at the onset of soot formation and therefore to gain additional understanding of the corresponding reaction pathways. Operation of the mass spectrometer as a mass filter allowing for measurement of mass ranges instead of specific molecular masses in the MBMS study of both benzene flames investigated in the present work revealed a shift of the mass distribution to higher masses with increasing height above the burner and between the nearly sooting and the sooting flame [42,81].

The species assessed by this approach were believed to consist of polycyclic material but identification of specific compound was not possible. The goal of the present work was to extend the inventory of concentration profiles along the flame axis of stable and radical compounds, particularly PAH, formed under nearly sooting and sooting conditions. In several studies, kinetic models were tested using the nearly sooting benzene/oxygen/argon flame (ϕ=1.8, 10% argon) [61,62,82-84]. The extension of the available experimental data to larger PAH and their radicals is expected to contribute to the improvement of detailed kinetic models and allow for the description of PAH and, ultimately, soot growth consistent with physical and chemical reality.

The development of kinetic models is widely based on the comparison of model predictions with experimental data sets. In the case of disagreement, thermodynamic and kinetic property data are checked for incompleteness or errors and the model modified in order to achieve computed species concentrations closer to the experimental values. However, in the development of kinetic models based on consistent high quality thermodynamic and kinetic property data, the uncertainty of experimental data should be taken into consideration. For instance, temperature measurements in combustion environments are challenging and the variation of the temperature profile used as input for the modeling of premixed flames has been found to have a significant impact on model predictions [85]. The use of kinetic models is usually based on the assumption of ideal experimental conditions such as perfect mixing, plug flow or unidimensional flames. In most cases, some deviation from these assumptions is inherent even to the best experimental equipment. For example, radial variation of temperature and species concentrations has been observed in unidimensional flat flames [86]. In the present work, in addition to the use of modified equipment initially built for MBMS studies [40,42,78], the experimental setup developed for radical scavenging with DMDS by Homann and co-workers [43,50,75-77], was transferred to our laboratory and also served for the investigation of the nearly sooting benzene flame. This unique opportunity allowed for the comparison of structures of a selected flame measured independently with two different setups but using the same sampling technique. All samples were analyzed using the same state-of-the chromatographic methods allowing for the identification of a large number of PAH including isomers [87-89]. If commercially not available, standard compounds necessary for the unambiguous identification of some PAH or the scavenging products, were synthesized by means of methods developed in the laboratory of a subset of the authors [90-92].

Details of the experimental setup developed in our laboratory, sample preparation and analysis and methods for the synthesis of standard compounds are given below. Results are presented and discussed in the context of PAH growth and soot formation. Data obtained by means of both setups using radical scavenging are compared with concentration profiles, if available, measured previously using MBMS [42]. This approach allows for the assessment of uncertainties inherent to one specific technique. In addition, it allows the validity of the calibration procedure used previously for large species such as PAH [42] to be checked.

Experimental Setup

Combustion Chamber and Sampling

Premixed flat flames were stabilized at 20 torr on a water-cooled drilled copper burner, 71 mm in diameter. A schematic of the experimental setup is given in **Fig. 1** while flame conditions are listed in **Table I**. The flames were sampled by a water-cooled 40°-90° hybrid quartz probe with a 0.7 mm orifice and expanded rapidly into a near vacuum environment (≈10^{-4} torr) forming a nozzle beam. Under these conditions, the mean free path for collisions is more than 1 meter. Therefore, bimolecular collisions are negligible and radicals stay in the gas stream without reaction subsequent to sampling. The vacuum was maintained by two 6'' diffusion pumps. The system was the built from a previous MBMS [40,42,78] by removing the skimmer and third vacuum stage. The flame gases are finally frozen upon impacting the "cold trap", which consists of two concentric cones, with the outside one opened to let the gases in. The trap was held at liquid nitrogen temperature, i.e., at 77 K. The cooling is ensured by liquid nitrogen passing through coils welded to the sides and the top of the trap. Scavenger, i.e., dimethyl disulfide, was added through a "scavenger feed doughnut", a ¼-inch tube formed in a circle and perforated with 14 equally spaced 0.5 mm holes at a 45 ° angle upward from the center (**Fig. 1**). This "scavenger feed doughnut" evenly distributed dimethyl disulfide across the surfaces of the cold trap and radicals sampled from the flame were stabilized via the following reaction: (1) $R\bullet + CH_3SSCH_3 \rightarrow R\text{-}SCH_3 + CH_3S\bullet$

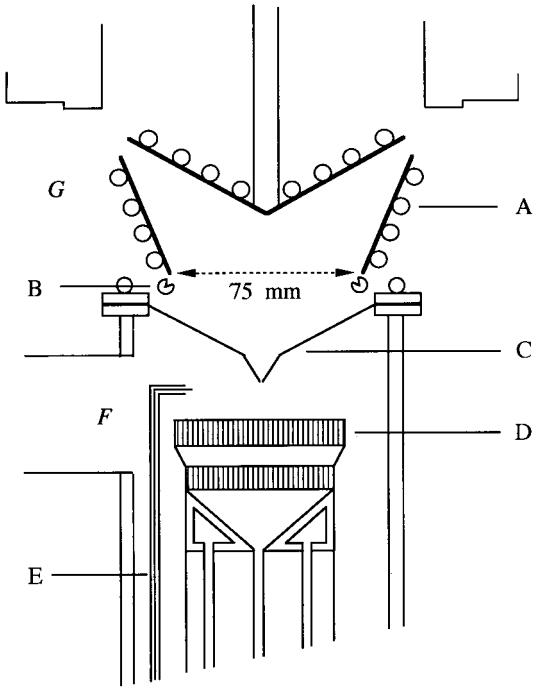

Fig. 1 Experimental setup, burner and scavenging system: **A** Cooling coils, **B** Vacuum chamber, **C** Quartz probe, **D** Burner, **E** Burner chamber, **F** Ignitor

In addition to the thiomethyl products of the scavenging reactions ($R\text{-}SCH_3$), all but the lightest flame gases (such as H_2, CO, O_2) are collected in the cold trap. Therefore other species, particularly PAH such as the parent molecules of the scavenged radicals, are available for subsequent analysis. Dimethyl disulfide, liquid at standard conditions, was vaporized by exposing it to the vacuum system through the feed doughnut. Critical flow was maintained across the holes of the feed doughnut, so the flow could be calibrated and controlled by the upstream pressure. The flow of scavenger was set at 3×10^{18} molecules per second,

Table I Experimental conditions

Flame	Equivalence ratio (ϕ)	Dilution (% Ar)	Pressure (torr)	Cold gas velocity (cm s^{-1})
I (nearly sooting)	1.8	30	20	50
II (slightly sooting)	2.0	30	20	50

compared to the total flow of flame gases through the probe of approximately 2×10^{19} molecules per second. Using similar sampling setup and conditions, Hausmann et al. [43] showed that increasing the dimethyl disulfide flow did not affect the concentration of thiomethyl products. Therefore, it is believed that radical species present in the sampling stream reacted nearly quantitatively with the scavenger.

In the present work, the possibility of analytical artifacts due to hydrogen displacement reactions of the thiomethyl radical ($CH_3S\bullet$) remaining after the initial scavenging reaction (1) was ruled out:

(2) $R\text{-}H + CH_3S\bullet \rightarrow R\text{-}SCH_3 + H$

Perdeuterated naphthalene ($C_{10}D_8$) was mixed with the scavenger and fed to the cold trap while sampling a flame as described above. Though large amounts of $C_{10}D_8$ were found in the resulting sample, no $C_{10}D_7SCH_3$ was identified. In agreement with thermodynamic calculations reported by Hausmann and Homann [93], it was therefore concluded that all thiomethyl species present stem from radicals collected in the flame. The flow through the probe, necessary for the conversion of the sample composition to mole fractions, was determined experimentally by measuring the rate of pressure increase in the isolated vacuum chamber downstream of the probe.

Chemical Analysis

The cold trap was maintained at liquid nitrogen temperature (77 K), as the sampling of the continued for 45 min. After extinction of the flame, the system was brought to atmospheric pressure by adding desiccated nitrogen gas. The cold trap was raised into a sealed glove box and placed over a glass jar containing a small amount of dichloromethane (DCM) and shielded from light by aluminum foil. The cooling liquid nitrogen flow was halted and the trap was allowed to warm. Warmed scavenger and flame compounds dripped from the trap into the jar and were dissolved in DCM, keeping evaporation and precipitation of flame compounds to a minimum. After 30 min, the trap was rinsed with DCM in order to collect the remaining substances adhered to the trap. The volume of the collected sample, including the solvent, totaled ≈ 40 mL. An internal calibration standard consisting of a known volume (50 – 100 μL) of a prepared solution of perdeuterated PAH, including styrene (C_8D_8), naphthalene ($C_{10}D_8$), acenaphthene ($C_{12}D_{10}$), anthracene ($C_{14}D_{10}$), and pyrene ($C_{16}D_{10}$) was added to the sample. The use of internal standards allowed for the determination of the total amount of each compound without knowing the sample volume or injection volume and therefore reduces potential uncertainties. The analysis were conducted by means of gas chromatography coupled to mass spectrometry (GC-MS) using Hewlett-Packard (Rockville, MD) HP 5890 Series II Plus chromatograph in conjunction with a mass selective detector HP 5972. A 50% cross-linked phenyl-methyl-silicone capillary column that had a length of 30 m and an inner diameter of 0.25 mm (HP50+, Hewlett-Packard, Inc.) was used as stationary phase. Helium carrier gas flow was 1.0 mL min^{-1}. The injector temperature was 250 °C and the interface to the detector was maintained at 280 °C. Injection volume was in all cases 1.0 μL. The temperature program consisted of a hold at 50 °C for 1.5 min, followed by a linear ramp to 310 °C at 8 °C min^{-1} and a final hold at 310 °C for 5 min.

After analysis of the above described solution consisting of sample and internal standards, two additional injections were made following the reduction of the sample volume to ≈ 3 mL and 0.1 to 0.2 mL, respectively. For this purpose high purity nitrogen was blown over the sample,

evaporation some of the DCM. This approach allows increasing the precision of the chemical analysis of compounds with concentrations close to the detection limit in the initial sample.

Separately, a standard solution containing 34 PAH as well as the internal standard was prepared in 5 different dilutions and injected into the GC-MS in triplicate. The molecular ion for each compound was extracted from the chromatogram, the resulting peak was integrated and calibration curves were constructed relating peak area to concentration. The resulting expressions could be used for the determination of absolute amounts of all calibrated compounds present in the sample collected from the flame. No determination of the sample volume was necessary, since the quantity of internal standards added was known. The absolute amounts of species collected from the flame was converted to mole fractions taking into account the flow through the probe during the collection time and the cold trap collection efficiency, ε.

To calculate ε, a flow of argon and 3% benzene was sent through the burner while the sampling system was operated as if sampling a flame. Sample treatment and analysis was similar to that described above but toluene was added as internal standard. Taking into account the flow through the probe, ε was calculated to be 64 ± 5%. As an additional test, a sooting flame was sampled with the cold trap replaced by a large sheet of perforated paper. After 20 min, the paper exhibited a circular pattern of the soot particles, 60 to 80% of which would have impacted the cold trap. Since the collection efficiency of benzene was found to be within this range, it was deduced that ε is largely independent of the molecular mass and it was considered to be within the experimental error to assume that all compounds of interest had the same collection efficiency as benzene.

In cases where no or insufficient quantities of standards have been available, concentrations were determined by assuming that the calibration curves were the same as those for a compound of similar structure. For instance, all four acenaphthyl isomers were synthesized in house and GC-MS analysis showed their retention times and mass spectrometric fragmentation patterns to be significantly different. Based on this information, all four acenaphthyl isomers could be unambiguously identified to be present in samples collected from flames but due to the limited quantities available for the corresponding 1-, 3-, 4- and 5-methylthioacenaphthylene, the calibration curve determined for 2-menthylthionaphthalene was used. All species found to be present, the approach used for identification and calibration are listed in Table II. In addition, peak mole fractions in both investigated benzene/oxygen flames, i.e., at equivalence ratio of ϕ= 1.8 and 2.0, are provided. Also, peak mole fractions of species measured in the independent control experiment for the ϕ= 1.8 case using the equipment developed and built by the Homann group are given. Mole fraction profiles and the effect of the variation of the equivalence ratio are discussed below. Also, in some complex cases such as the identification of 1-, 2-, and 4-pyrenyl, additional information about the analytical procedure is provided. Details of the synthesis of 1-, 3-, 4- and 5-methylthioacenaphthylene are given. Acenaphthylene has been found to be abundant in flames, its radicals are therefore key intermediates in the further growth to PAH of increasing size and, based on our best knowledge, mole fraction profiles of individual acenaphthyl radicals have not been reported previously.

Syntheses of Authentic Thiomethylacenaphthylenes

The four thiomethylacenaphthylenes necessary for the unambiguous identification of acenaphthyl radicals, were synthesized in an isomer-specific manner in the laboratory of Prof. L. T. Scott in the Department of Chemistry at Boston College. The corresponding haloacenaphthylenes, all of which previously known compounds, were used as starting materials.

Thus, treatment of 1-bromoacenaphthylene [94-96] with sodium thiomethoxide ($NaSCH_3$) in the dipolar aprotic solvent 1,3-dimethyl-2-imidazolidinone (DMEU) gave 1-thiomethylacenaphthylene. Analogous treatment of 3-chloroacenaphthylene [97] and 5-bromoacenaphthylene [98] with sodium thiomethoxide gave 3-thiomethylacenaphthylene and 5-thiomethylacenaphthylene, respectively.

The yields of these nucleophilic substitution reactions are relatively modest (43 – 56%) because direct addition of sodium thiomethoxide to the 5-membered ring double bond generates byproducts containing two thiomethyl groups. The nucleophilic substitution reaction fails completely on 4-bromoacenaphthylene [99] and gives only the product of sodium thiomethoxide addition to the 5-membered ring double bond.

To circumvent this complication, an alternative strategy was employed for the preparation of 4-thiomethylacenaphthylene. Thus, 4-bromoacenaphthylene was converted first to 4-lithioacenaphthylene by bromium/lithium exchange with n-butyllithium in tetrahydrofuran at –78 °C, and the thiomethyl group was then introduced using the electrophilic reagent dimethyldisulfide [100]. The 1H NMR and mass spectra of all four thiomethylacenaphthylenes are completely consistent with the structures assigned.

Results

In all, 54 aromatic species including 12 radicals were measured in the present work (Table II). Selected compounds which are believed to be essential for the formation of PAH of increasing size and ultimately of soot, are discussed below. Mole fraction profiles as a function of the height above the burner (HAB) are given. Uncertainties are assessed by comparison with independent control experiments conducted using the experimental setup developed and built by the Homann group [76,77] and in some cases with the MBMS data of Bittner and Howard [42]. In the nearly sooting benzene flame (ϕ= 1.8), mole fractions at 0.30, 0.40, 0.50, 0.58, 0.59, 0.67, 0.69, 0.74, 0.80, 0.88, 0.94, 1.00, 1.05 and 1.09 cm from the burner were measured. No PAH could be identified at higher heights above the burner, at least partially due to PAH consumption by subsequent growth reactions [61]. Additional data points reported by Benish [79] at HAB= 0.76 and 0.78 cm have been omitted after a careful revisit of all available information. The sooting benzene flame of ϕ= 2.0 has been mainly investigated in order to access the impact of the equivalence ratio on concentrations of PAH and their radicals. Therefore samples were only taken at locations where concentrations close to the maxima were expected, i.e., at HAB= 0.76, 0.81, 090, 0.93 and 1.00 cm.

Single-Ring Aromatics

The formation unstable benzene derivatives such as phenyl and phenoxy was found to be dominant in the early stage of benzene degradation in flames [85]. Stabilization of phenoxy by reaction with H radicals was found to be the dominant phenol formation pathway in the benzene/oxygen flame of ϕ= 1.8 studied here [85]. Besides hydrogen abstraction with OH, unimolecular decomposition to cyclopentadiene (C_5H_6) and CO was the only important phenol consumption pathway identified [85]. Depending on the equivalence ratio, phenyl can be oxidized, for instance by reaction with molecular oxygen and decay subsequently by unimolecular reactions or form substituted one-ring aromatics such as phenylacetylene ($C_6H_5C_2H$) and styrene ($C_6H_5C_2H_3$) which are precursors of PAH of increasing size [63,64].

(1) $C_6H_5 + O_2 \leftrightarrows C_6H_5O + O$

(2) $C_6H_5O \leftrightarrows C_5H_5 + CO$

(3) $C_6H_5O + H \leftrightarrows C_6H_5OH$
(4) $C_6H_5OH \leftrightarrows C_5H_6 + CO$
(5) $C_6H_5 + C_2H_2 \leftrightarrows C_6H_5C_2H + H$
(6) $C_6H_5 + C_2H_4 \leftrightarrows C_6H_5C_2H_3 + H$

In the present work, methylthiobenzene ($C_6H_5SCH_3$), benzylmethylsulfide ($C_6H_5CH_2SCH_3$), phenol, phenylacetylene and styrene were identified unambiguously by means of the match of retention times and fragmentation patterns of authentic standards. Based on the assumption of complete conversion of phenyl radicals after collection, discussed above, the amounts of methylthiobenzene and benzylmethylsulfide were considered to reflect the quantities of phenyl and benzyl ($C_6H_5CH_2$), respectively, collected from the flame. Benzyl has been suggested to contribute to naphthalene formation via in reaction with propargyl [34]. Mole fraction profiles were established and those of phenyl, benzyl and phenylacetylene are shown in **Fig. 2**. The measurement of phenyl by means of the radical scavenging technique is of particular interest because it allows assessing the importance of phenyl in benzene combustion in comparison to its isomers such as fulvene radicals. Fulvene () was suggested to play a significant role in benzene formation [101] but the absence of identifiable quantities of fulvene radicals allows to rule out their contribution to benzene consumption under the conditions studied in the present work. Comparison with control experiment conducted with the experimental setup developed and built by the Homann group [76,77] and using a similar procedure for sample preparation and analysis shows a ≈ 2-fold higher peak mole fraction in the modified MIT equipment [79] while peak location and shape were identical (**Table II**). The MBMS profile measured by Bittner and Howard [42] using the original equipment revealed a peak mole fraction ≈ 10% higher than the control experiment but is thought to be less precise than the radical scavenging technique. Comparison of mole fraction profiles of stable single-ring aromatics, i.e., phenol, styrene and phenylacetylene with the control experiment and MBMS data [42] showed nearly identical shapes and peak locations and values.

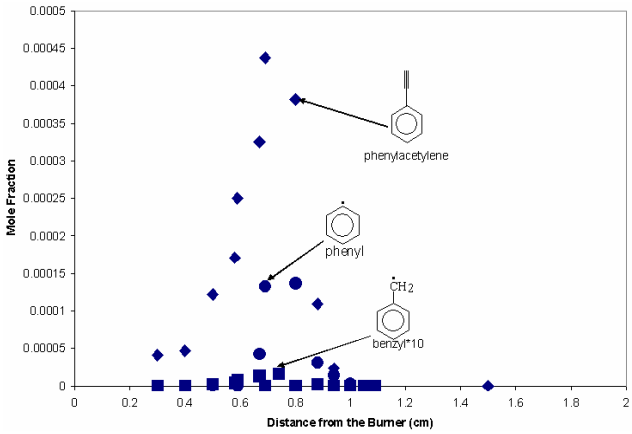

Fig. 2 Experimental mole fraction profiles in the nearly sooting laminar premixed benzene/oxygen/argon flame (ϕ= 1.8, 30% argon, cold gas velocity v= 50 cm s^{-1}, 20 torr). ● : phenyl, ■ : benzyl (× 10) and ◆ : phenylacetylene.

The compared to stable species higher uncertainty of absolute values of the radical species is consistent with the significant challenge of the measurement and therefore not surprising.

The comparison with the ϕ= 2.0 flame does show no significant impact of the equivalence ratio on shape, peak value of single-ring aromatics. No clear trend was observed, discrepancies were ± 25%, i.e., clearly within the expected uncertainty of the measurement. However, mole fraction profiles were shifted by ≈ 2 mm towards the burned gases.

Table II Peak mole fractions

Species	$X_{maximal}$	$X_{max.}$ (control)	[42]
Phenyl	$1.4\ 10^{-4}$	$6\ 10^{-5}$	$7.45\ 10^{-5}$
Phenol	$1.3\ 10^{-3}$	$1.2\ 10^{-3}$	-
Phenylacetylene	$4.0\ 10^{-4}$	$3.8\ 10^{-4}$	$4.0\ 10^{-4}$
Styrene	$7.0\ 10^{-5}$	$5.0\ 10^{-5}$	$3.2\ 10^{-5}$
Naphthalene	$2.4\ 10^{-4}$	$8\ 10^{-5}$	$1.0\ 10^{-4}$
1-naphthyl	$2.5\ 10^{-6}$	$1.3\ 10^{-6}$	-
2-naphthyl	$3.0\ 10^{-6}$	$1.8\ 10^{-6}$	-
2-vinylnaphthalene	$1.9\ 10^{-6}$	$1.0\ 10^{-6}$	-
Biphenyl	$8.0\ 10^{-5}$	$6.0\ 10^{-5}$	-
Sum $C_{12}H_{10}$	$8.2\ 10^{-5}$	$6.1\ 10^{-5}$	$1.5\ 10^{-5}$
2-methylnaphthalene	$2.0\ 10^{-5}$	$1.0\ 10^{-5}$	-
1-ethynylnaphthalene	$1.2\ 10^{-5}$	$2.0\ 10^{-6}$	-
2-ethynylnaphthalene	$3.0\ 10^{-5}$	$1.7\ 10^{-5}$	-
Biphenylene	$1.5\ 10^{-6}$	$1.2\ 10^{-6}$	-
acenaphthylene	$1.2\ 10^{-4}$	$3.8\ 10^{-5}$	-
Sum $C_{12}H_8$	$1.64\ 10^{-4}$	$5.82\ 10^{-5}$	-
1-acenaphthyl	$2.2\ 10^{-7}$	$8\ 10^{-8}$	-
3-acenaphthyl	$1.1\ 10^{-7}$	$5\ 10^{-8}$	-
4-acenaphthyl	$9\ 10^{-7}$	$7\ 10^{-7}$	-
5-acenaphthyl	$2\ 10^{-7}$	$1\ 10^{-7}$	-
Indene	$1.7\ 10^{-4}$	$1.5\ 10^{-4}$	$1.5\ 10^{-4}$
1-ethynylacenaphthylene	$1.0\ 10^{-5}$	$5.0\ 10^{-6}$	-
5-ethynylacenaphthylene	$1.1\ 10^{-5}$	$1.0\ 10^{-6}$	-
Sum $C_{14}H_8$	$2.2\ 10^{-5}$	$6.0\ 10^{-6}$	$7.0\ 10^{-6}$
1-phenylnaphthalene	$1.3\ 10^{-6}$	$6.0\ 10^{-7}$	-
2-phenylnaphthalene	$2.2\ 10^{-6}$	$1.4\ 10^{-6}$	-
Phenanthrene	$2.3\ 10^{-5}$	$9.0\ 10^{-6}$	-
Anthracene	$4.0\ 10^{-6}$	$1.5\ 10^{-6}$	-
Sum $C_{14}H_{10}$	$2.7\ 10^{-5}$	$1.05\ 10^{-5}$	$6.0\ 10^{-6}$
Fluoranthene	$1.2\ 10^{-5}$	$4.5\ 10^{-6}$	-
Pyrene	$1.2\ 10^{-5}$	$4.0\ 10^{-6}$	-
Acephenanthrylene	$6.0\ 10^{-6}$	$1.5\ 10^{-6}$	-
Sum $C_{16}H_{10}$	$3.0\ 10^{-5}$	$1.0\ 10^{-5}$	$3.0\ 10^{-6}$
cyclopenta[cd]pyrene	$6.0\ 10^{-6}$	$1.2\ 10^{-6}$	-
benzo[ghi]fluoranthene	$3.5\ 10^{-6}$	$1.0\ 10^{-6}$	-
benzo[a]anthracene	$7.0\ 10^{-7}$	$2.0\ 10^{-7}$	-
Chrysene	$1.0\ 10^{-6}$	$3.0\ 10^{-7}$	-
benzo[b]fluoranthene	$2.0\ 10^{-7}$	$3.0\ 10^{-8}$	-
benzo[k]fluoranthene	$1.0\ 10^{-7}$	$5.0\ 10^{-9}$	-
benzo[a]pyrene	$1.8\ 10^{-7}$	$3.0\ 10^{-8}$	-
indeno[1,2,3-cd]pyrene	$8.0\ 10^{-8}$	$2.0\ 10^{-8}$	-
benzo[ghi]perylene	$1.0\ 10^{-7}$	$8.0\ 10^{-8}$	-
1-naphthol	$9.0\ 10^{-6}$	$1.2\ 10^{-6}$	-
2-naphthol	$7.5\ 10^{-6}$	$2.5\ 10^{-6}$	-

Two-Ring Aromatics

Increasing size of PAH adds as additional challenge the presence of isomers. In the present work, 1- and 2-naphthyl radicals could be distinguished and 2-methylnaphthalene, 2-vinylnaphthalene, 1- and 2-ethynylnaphthalene, 1- and 2-naphthol were unambiguously identified. In addition, both phenyl-substituted naphthalenes, i.e., 1- and 2-phenylnaphthalene were measured. Also, profiles of naphthalene, an isomer to diethynylbenzene (not identified), biphenyl which has the same molecular mass as vinylnaphthalenes and indene were obtained in the present work. Authentic standards were used for the identification and quantification of all two-ring aromatics, cited above, except 1-naphthol which has been estimated from its fragmentation pattern and was calibrated assuming the same response factor as 2-naphthol.

Naphthalene, its radicals and biphenyl have been found to play a significant role in the formation of larger PAH such as acenaphthylene [64] and phenanthrene [102]. 1- and 2-ethynylnaphthalene are intermediates in the formation of phenanthrene and anthracene via the hydrogen-abstraction/acetylene-addition (HACA) pathway and their mole fraction profiles are expected to be valuable for the assessment of the contribution of the HACA mechanism by means of detailed kinetic modeling. Methyl- [34,42] and vinyl- [102] substituted compounds might contribute to PAH growth under certain conditions. Similar to phenol, 1-, 2-naphthol and 1-, 2-naphthoxy, the latter ones not identified experimentally, are products of the oxidation of

naphthalene and 1- and 2-naphthyl and they are thought to decay to indene and indenyl [61]. In a recent modeling study [62], the previous measurement of mole fraction profiles of 1- and 2-naphthyl radicals using the radical scavenging technique [79] allowed for the identification of the reaction of phenylacetylene radicals ($C_6H_5C_2H$*2) with acetylene to 1-naphthyl, i.e., (7) $C_6H_5C_2H$*2 + C_2H_2 ⇆ 1-naphthyl, as a consumption pathway of two-ring aromatics in the benzene flame at ϕ= 1.8, also studied here. 1-phenylnaphthalene is a likely precursor of fluoranthene, containing a five-membered ring, while hydrogen-abstraction/acetylene addition of 2-phenylnaphthalene leads to the formation of chrysene. Mole fraction profiles of naphthalene, 1- and 2-naphthyl, 1- and 2-ethynylnaphthalene and 2-vinylnaphthalene in the nearly sooting benzene flame of ϕ= 1.8 are given **in Fig. 3 and 4**. 1-ethynylnaphthalene is a potential precursors of acenaphthylene and – after an additional hydrogen-abstraction/acetylene-addition sequence – of phenanthrene. Hydrogen-abstraction/acetylene-addition beginning with 2-ethynylnaphthalene can lead to the formation of phenanthrene or anthracene depending on the site of hydrogen abstraction. A detailed study of the potential energy surface of 1-naphthyl + acetylene followed by the determination of kinetic data for different temperatures and pressures allowing for the quantitative assessment of the competition between different reaction channels was conducted recently [103]. The comparison with the control experiments in the setup provided by the Homann group, showed typically discrepancies between 10% and three-fold. In all cases, peak mole fractions were lower in the control experiments. This observation might be related to a limited reproducibility of equivalence ratios, particularly challenging in the case of liquid fuels but also to different cooling of the burners. For two species, 1-ethynylnaphthalene and 1-naphthol, a six to seven-fold higher peak mole fraction than in the control experiment was found. This lack of agreement might be related to retention times very close to those of the corresponding 2- isomers (only separated by 0.1 min, respectively), overlaps between these isomers can therefore not be excluded.

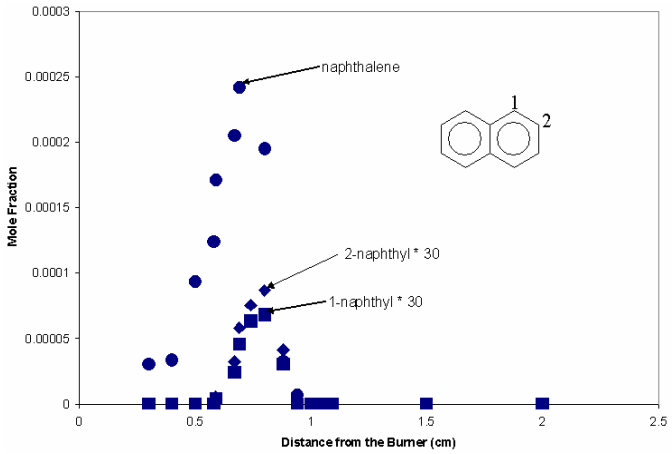

Fig. 3 Experimental mole fraction profiles in the nearly sooting laminar premixed benzene/oxygen/argon flame (ϕ= 1.8, 30% argon, cold gas velocity v= 50 cm s^{-1}, 20 torr). ● : naphthalene, ■ : 1-naphthyl (× 30), ◆ : 2-naphthyl (× 30).

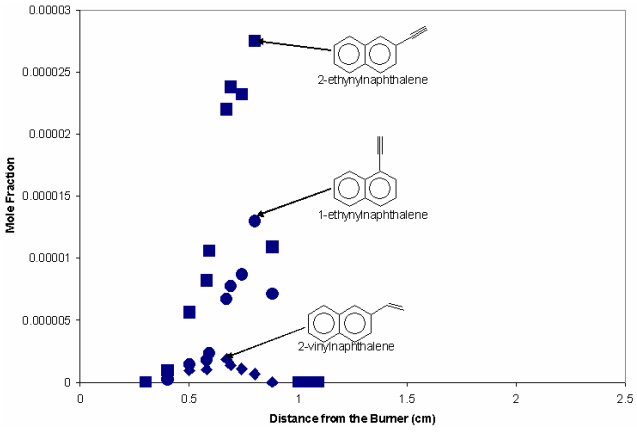

Fig. 4 Experimental mole fraction profiles in the nearly sooting laminar premixed benzene/oxygen/argon flame (ϕ= 1.8, 30% argon, cold gas velocity v= 50 cm s^{-1}, 20 torr). ● : 1-ethynylnaphthalene, ■ : 2-ethynylnaphthalene, ◆ : 2-vinylnaphthalene.

Mole fraction profiles for naphthalene and 1- and 2-naphthyl radicals in the slightly sooting flame of ϕ= 2.0 are given in **Fig. 5**. Similar to single-ring aromatics, no significant and consistent impact of the increase of the equivalence ratio on peak mole fractions could be observed for aromatic containing two aromatic rings while mole fraction profiles were shifted by ≈ 2 mm towards the burnt gases.

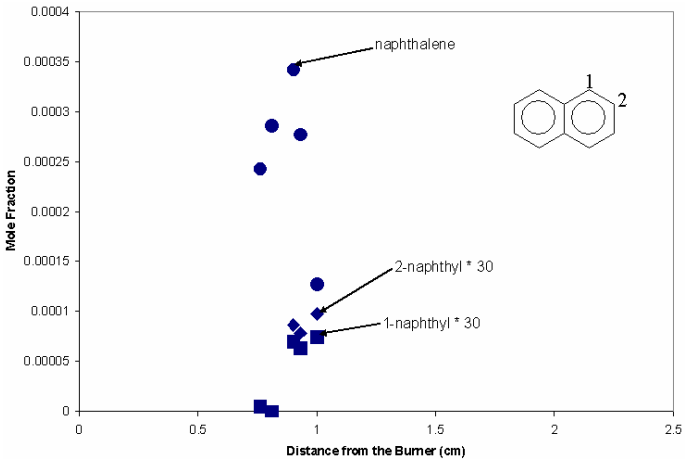

Fig. 5 Experimental mole fraction profiles in the slightly sooting laminar premixed benzene/oxygen/argon flame (ϕ= 2.0, 30% argon, cold gas velocity v= 50 cm s^{-1}, 20 torr). ● : naphthalene, ■ : 1-naphthyl (× 30), ◆ : 2-naphthyl (× 30).

Three-Ring PAH

A significant number of PAH containing three condensed rings has been identified. Isomers such as phenanthrene and anthracene exist and in addition to condensed six-membered rings, also species containing five-membered and four-membered rings, i.e., acenaphthylene and biphenylene, have been observed. The characteristics of C-H bonds are expected to depend significantly on the location in the molecule. For instance, the structural environment of the C-1 carbon in acenaphthylene is likely to be different from those of carbon atoms in the system of condensed hexagons and density functional theory computations showed the energy of homolytic C-H bond cleavage of phenanthrene to be ≈ 2 kcal $mole^{-1}$ smaller at the relatively congested C-4 position than at all other carbons [104].

Fluorene, biphenylene, acenaphthylene, phenanthrene and anthracene were identified by means of authentic standards. Mole fraction profiles of the four latter species measured in the flame at ϕ= 1.8 are shown in **Fig. 6**. 1- and 5-ethynylacenaphthylene, i.e., two of five ethynylacetylenes, could be synthesized and allowed for their unambiguous identification and quantification in the samples collected from the flames. 1-ethynylacenapthylene is a potential precursor of fluoranthene while 5-ethynylacenaphthylene can lead to cylcopenta[cd]pyrene via two hydrogen-abstraction/acetylene-addition steps. Similar to the competition between the formation of 1-ethynylnaphthalene and acenaphthylene [62,103], reaction of 5-acenaphthyl with acetylene is expected to give besides 5-ethynylacenaphthylene pyracylene. However, no pyracylene could be identified. The stability and therefore its lifetime of pyracylene after its

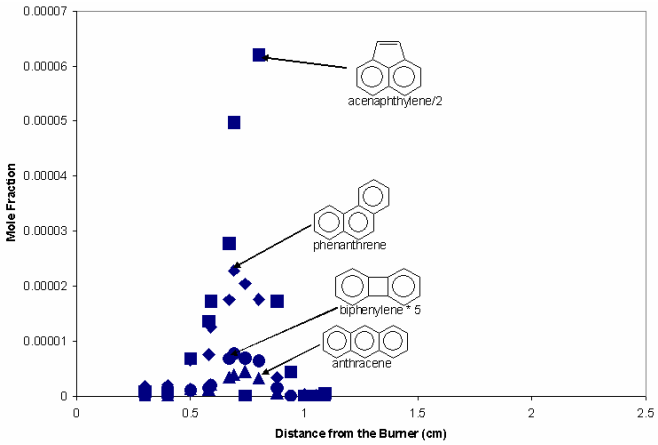

Fig. 6 Experimental mole fraction profiles in the nearly sooting laminar premixed benzene/oxygen/argon flame (ϕ= 1.8, 30% argon, cold gas velocity v= 50 cm s^{-1}, 20 torr). ● : biphenylene (× 5), ■ : acenaphthylene (× 0.5), ◆ : phenanthrene, ▲ : anthracene.

synthesis were found to be limited, i.e., composition after sampling after prior analysis can not be excluded. At the current stage, no definitive conclusion about the presence of pyracylene is possible. Two additional gas chromatographic peaks, partially co-eluting, of species of a mass 176 amu were identified. Due to their retention times and fragmentation pattern similar to those of 1- and 5-ethynylacenaphthylene, these peaks are believed to stem from 3- and 4-ethynylacenaphthylene. One of these compounds was found to be the most abundant ethynylacenaphthylene isomer with a peak mole fraction approximately twice as high as that of 1-ethynylacenaphthylene.

The scavenging products of all four acenaphthylene radicals were identified by means of authentic standards synthesized in the present work using the procedure described above. The quantification of all isomers was conducted based on the chromatographic response factor of 2-methylthioacenaphthylene and the mole fraction profiles of 1-, 3-, 4- and 5-acenaphthyl were determined following the procedure, described above (**Fig. 7**). The radical at the 4-position was over three times more prevalent than 1- and 5-acenaphthyl and nearly 10 times more abundant than the C-3 radical. These pronounced differences in the relative abundances of acenaphthyl radicals do not correlate with thermodynamic property data, discussed below, and are therefore likely to be kinetically driven.

The comparison with the control experiments shows a mixed picture for the peak mole fractions while good agreements for shapes and peak locations were observed in all cases. Good to fair agreements, i.e., less than ≈ 2-fold discrepancies, were found for biphenylene, 3-, 4- and 5-acenaphthyl and 1-ethynylacenaphthylene while between 2- and 5-fold lower peak mole fractions were observed in control experiments for acenaphthylene, 1-acenaphthyl, phenanthrene and anthracene. The compared to the control experiment ≈10-fold higher peak mole fraction of 5-ethynylacenaphthylene might be related to its partial co-elution with ethynylacenaphthylene isomers in the gas chromatographic analysis. Therefore, a lower peak mole fraction of 5-ethynylacenaphthylene cannot be excluded. No phenanthryl and anthracyl radicals could be identified in the original work [79]. However, analysis of samples collected in the control experiments showed peaks with molecular masses and fragmentation patterns consistent with the scavenging patterns of phenanthryl and anthracyl scavenging products. No assignment of peaks to specific compounds was possible due to the lack of authentic standards and peak mole fractions of approximately 1.5 to 5 10^{-8} were estimated.

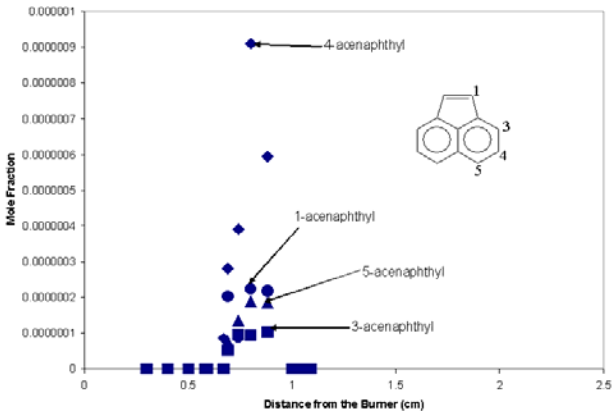

Fig. 7 Experimental mole fraction profiles in the nearly sooting laminar premixed benzene/oxygen/argon flame (ϕ= 1.8, 30% argon, cold gas velocity v= 50 cm s^{-1}, 20 torr). ● : 1-acenaphthyl, ■ : 3-acenaphthyl, ◆ : 4-acenaphthyl, ▲ : 5-acenaphthyl.

Similar to single- and two-ring aromatics, the comparison of mole fraction profiles measured in the benzene flames at ϕ= 1.8 and 2.0 showed a shift of the peak location by ≈ 2 mm towards the postflame zone in the latter case. Different from one- and two-rings containing compounds, up to two-fold higher peak mole fractions were observed in the slightly sooting (ϕ= 2.0) in

comparison to the nearly sooting (ϕ= 1.8) flames. This finding might indicate the contribution of three-ring PAH to soot formation.

Four-Ring PAH

All species with the molecular formulas $C_{16}H_{10}$, i.e., pyrene, fluoranthene, acephenanthrylene, aceanthrylene and $C_{18}H_{12}$, i.e., chrysene, benzo[a]anthracene were identified in both nearly sooting and slightly sooting benzene flames. Mole fraction profiles of all $C_{16}H_{10}$ isomers in the nearly sooting benzene flame (ϕ= 1.8) are shown in **Fig. 8**. Previous studies of ethylene combustion with naphthalene injection in a well-stirred-plug-flow reactor setup have shown the approach of equilibrium conditions between isomers of containing five-membered rings such as fluoranthene, acephenanthrylene and aceanthrylene or cyclcopenta[cd]pyrene and benzo[ghi]-fluoranthene [105]. This finding is consistent with the evidence of thermal interconversions of aceanthrylene, acephenanthrylene and fluoranthene [106]. In addition, mole fraction profiles cyclopenta[def]phenanthrene were measured in both flames.

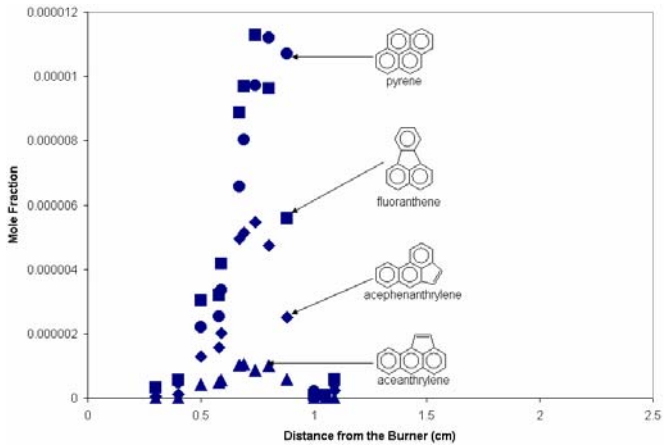

Fig. 8 Experimental mole fraction profiles in the nearly sooting laminar premixed benzene/oxygen/argon flame (ϕ= 1.8, 30% argon, cold gas velocity v= 50 cm s^{-1}, 20 torr). ● : pyrene, ■ : fluoranthene, ◆ : acephenanthrylene, ▲ : aceanthrylene.

A group of five small chromatographic peaks followed by three larger ones with fragmentation patterns consistent with the scavenging products of pyrenyl and fluoranthyl radicals were identified all within 1 min retention time. Consistent with the compared to pyrene smaller retention time of fluoranthene and the existence of five different radical sites in the case of fluoranthene and three in that of pyrene, the first group of peaks was assigned to methylthiofluoranthenes, followed by methylthiopyrenes. This assumption was confirmed by the use of 5-methylthiofluoranthene and 1-methylthiopyrene, synthesized in the present work, as authentic standards. The gas chromatographic peak of 5-methylthiofluoranthene fell within the first group by retention time but due to the similarity of the fragmentation patterns, no unambiguous match with one of the detected species was possible. Therefore, only the mole fraction profile of the sum of all fluoranthyl radicals was reported in the present work (**Fig. 9**). 1-methylthiopyrene matched one of the peaks of the second

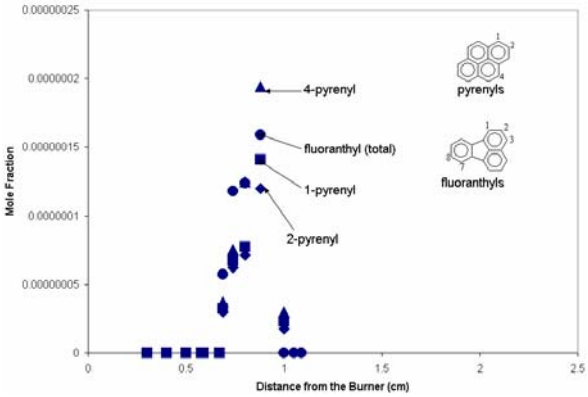

Fig. 9 Experimental mole fraction profiles in the nearly sooting laminar premixed benzene/oxygen/argon flame (ϕ= 1.8, 30% argon, cold gas velocity v= 50 cm s^{-1}, 20 torr). ● : fluoranthyl (total), ■ : 1-pyrenyl, ◆ : 2-pyrenyl, ▲ : 4-pyrenyl.

group by retention time and fragmentation pattern and, in consequence, a mole fraction profile of the 1-pyrenyl radical could be established (**Fig. 9**).

Attempts to assign the structures of the two remaining methylthiopyrenes from their fragmentation patterns were unsuccessful but the correlation between polarity and retention time could be used for identification. In fact, polar compounds should preferentially adhere to the GC column used in the present work and therefore elute later than less polar compounds of similar structure. The sulfur atoms of 1-methylthiopyrene and 4-methylthiopyrene, both attached adjacent to the junction of two six-membered rings, can easily form intramolecular hydrogen bonds and therefore effectively reduce the polarity of the compounds while no such hydrogen bond is possible in the case of 2-methylthiopyrene. Similar to the elution order of 1- and 2-methylthionaphthalene, 2-methylthiopyrene is therefore expected to elute later than its isomers. Based on this reasoning, mole fraction profiles of 2- and 4-pyrenyl radicals were established (**Fig. 9**).

Similar to PAH containing two and three rings, the control experiments showed consistently smaller peak mole fractions. Discrepancies for stable and radical species ranged from ≈ 2.5-fold in the case of fluoranthene to ≈ 3.5-fold for benzo[a]anthracene.

The impact of the increase of the equivalence ratio ϕ from 1.8 to 2.0 was similar to that observed for PAH containing three condensed rings. Peak mole fractions were ≈ 2 to 2.5-fold while the mole fraction profiles shifted by ≈ 2 mm towards to postflame zone.

PAH Containing Five and More Aromatic Rings

PAH containing up six condensed aromatic rings were identified and mole fraction profiles measured. Consistent with previous work in a sooting benzene/oxygen flame [47], a significant decrease in abundance was observed with increasing molecule size and therefore no scavenging products of these large PAH could be detected after a sampling time of 45 min. At least two of the identified five aromatic rings containing species, cyclopenta[cd]pyrene and benzo[a]pyrene were found to be mutagenic [7] while benzo[ghi]fluoranthene has been thought to play a role in the formation of fullerenes [107]. The detection of benzo[a]fluoranthene, benzo[k]fluoranthene and indeno[1,2,3-cd]pyrene illustrates the contribution of PAH to the growth process to PAH of increasing size via cyclodehydrogenation [108,109] or reactive dimerization [110]. Mole fraction profiles of cyclopenta[cd]pyrene, benzo[ghi]fluoranthene and benzo[ghi]perylene are given in **Fig. 10**. Overall and consistent with decreasing concentrations, comparison to the control experiments showed with molecular size increasing discrepancies of peak mole fractions. The control experiments showed in most cases ≈ 3 to 4 times lower peak values while significant larger uncertainties were observed for benzo[b]fluoranthene and benzo[k]fluoranthene. No profiles of these two compounds are therefore provided for the two latter species. However, an

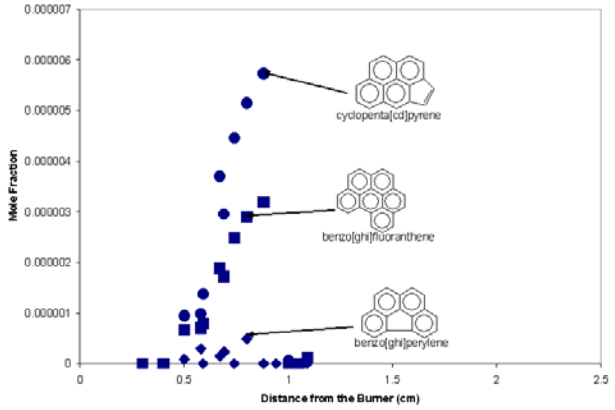

Fig. 10 Experimental mole fraction profiles in the nearly sooting laminar premixed benzene/oxygen/argon flame (ϕ= 1.8, 30% argon, cold gas velocity v= 50 cm s^{-1}, 20 torr). ● : cyclopenta[cd]pyrene, ■ : benzo[ghi]-fluoranthene, ◆ : benzo[ghi]perylene.

excellent agreement was found for benzo[ghi]perylene, the largest PAH the largest PAH measured in the present work, with a ≈ 20% higher peak mole fraction in the peak experiment.

The effect of the increase of the equivalence ratio ϕ from 1.8 to 2.0 was for some species such as benzo[a]pyrene, benzo[b]fluoranthene and benzo[k]fluoranthene more pronounced than for smaller PAH while a similar shift of the profiles ≈ 2 mm towards the postflame zone was observed. However, the more pronounced increase for some species should not be considered as a definitive conclusion because of the uncertainty of the experimental data assessed by the control experiments, discussed above.

Oxygenated PAH

In addition to phenol, 1- and 2-naphthol, already discussed, the following oxygenated PAH have been detected and quantified by means of authentic standards: Dibenzofuran, 1-acenapthenone, 9-fluorenone, phenalenone, benzanthrone and benzo[a]pyrenone. Oxygenated PAH have been found in size-segregated urban aerosols [111] and are expected to play a significant role as intermediates in the oxidative consumption of PAH [112]. The availability of data is expected to be of significant value for the investigation of PAH oxidation pathways. Mole fraction profiles of 1-acenaphthenone, benzanthrone and benzo[a]pyrenone measured in the ϕ= 1.8 benzene flame are given in **Fig. 11**. Consistent with the faster consumption of oxygen, no benzanthrone and benzo[a]pyrenone were identified in the flame with ϕ= 2.0. However, a ≈ 50% increase of the peak mole fractions was observed for the smaller oxy-PAH, as well as the ≈ 2 mm shift towards the postflame zone, already seen for all non-oxygenated PAH.

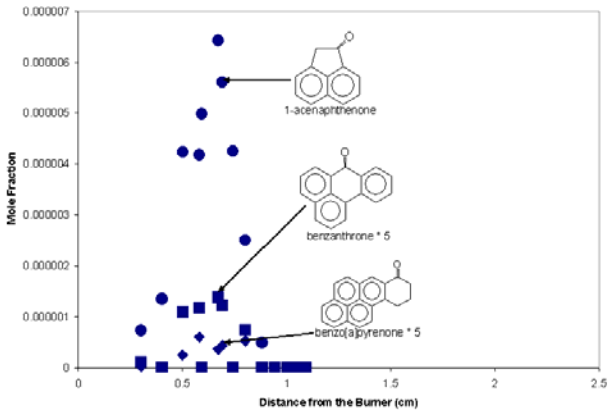

Fig. 11 Experimental mole fraction profiles in the nearly sooting laminar premixed benzene/ oxygen/argon flame (ϕ= 1.8, 30% argon, cold gas velocity v= 50 cm s^{-1}, 20 torr). ● : 1-acenaphthenone, ■ : benzanthrone (× 5), ◆ : benzo[a]pyrenone (× 5).

Equilibrium Calculations

The growth of PAH and ultimately to soot and fullerenes is a complex process in which thermodynamic considerations play a significant role. Many reactions are in a large extent thermodynamically driven but in addition energetically feasible reaction pathways are required to allow for the formation of specific products in the available time frame [2]. For instance, the investigation of thermodynamic driving forces for fullerene formation showed no insuperable thermodynamic barriers [113] while the use of a complex kinetic model did lead to a 50- to 100-fold underprediction of the experimental peak of C_{60} and C_{70} [61]. That illustrates that thermodynamics are a necessary but not always sufficient condition. Particularly in the postflame zone, i.e., at relatively high residence times, partial equilibrium is often reached for individual reactions and reaction subsystems [114,115].

The formation of PAH of increasing size and ultimately of soot by addition of growth species such as acetylene or PAH is initiated by the formation of PAH radicals via hydrogen abstraction with mainly H and OH radicals. The availability in the present work of mole fraction profiles of

PAH radicals and the corresponding PAH radicals in conjunction with those measured previously for H, H_2, OH and H_2O [42] allowed to check in which extent equilibrium has been reached.

Hydrogen abstraction with H and OH was investigated for naphthalene, acenaphthylene and pyrene, radical information available for all isomers.

(8) PAH + H ⇆ PAH• + H_2

(9) PAH + OH ⇆ PAH• + H_2O

Ratios of the experimental mole fractions between PAH radicals and their parent molecules were compared with the corresponding equilibrium conditions. Based on the equilibrium constants of rxn. (8) and (9), PAH radical to PAH ratios can be calculated by means of $X_{PAH\bullet}/X_{PAH} = K_8 \times (X_{H\bullet}/X_{H2})$ and $X_{PAH\bullet}/X_{PAH} = K_9 \times (X_{OH\bullet}/X_{H2O})$. The thermodynamic property needed for the determination of the equilibrium constants were taken form the literature or calculated by means of density functional theory followed by vibrational analysis using a procedure described previously [62,103]. Isodesmic reactions were used for the determination of heats of formation of radical species.

Experimental radical-parent mole fraction ratios were determined at the locations of maximum radical concentrations, i.e., at 0.80 cm from the burner for 1- and 2-naphthyl, 1-, 3-, 4- and 5-acenaphthyl and 0.88 cm for 1-, 2- and 4-pyrenyl. The corresponding equilibrium ratios were calculated at 1800 K using X_H= 0.00238, X_{H2}= 0.0727, X_{OH}= 0.0006385 and X_{H2O}= 0.1659 measured by means of MBMS [42] at 0.86 cm from the burner, the location of maximum PAH concentration in their study. Both experimental and calculated PAH radical – parent ratios are given in Table III. For all investigated radicals, peak concentrations are lower than predicted by the equilibrium. Equilibrium concentrations determined via hydrogen-abstraction with H, i.e., rxn. (8), are lower than those obtained based on hydrogen-abstraction with OH (rxn. (9)). An overall trend of approaching equilibrium with increasing size of the molecule can be observed but 3-acenaphthyl is a striking exception. A possible explanation might be related to other reactions involved in the growth and consumption process of PAH. Such reactions could be close to (or even beyond) partial equilibrium and therefore prohibitive for higher radical concentrations. For instance, butadiyne (diacetylene, C_4H_2), the second member of the series of polyacetylenes, previously discussed as key species in soot formation [1,2], was suggested by Hausmann and Homann [77] to be a product of PAH decomposition at high temperature. Based on the benzene ring contraction mechanism of Scott and coworkers [118], they developed a reaction scheme based on two isomerization reactions starting with 1-naphthyl followed by ring opening and decomposition to phenyl and butadiyne [77]. In the present work, the mole fraction ratio of 2-naphthyl to phenyl was calculated based on the assumption of partial equilibrium of

Table III Experimental radical to parent molecule mole fraction ratios compared to equilibrium.

Radical	$X_{radical}/X_{parent}$ [%], 1800 K	H-abstraction with H $X_{radical}/X_{parent}$ [%]	H-abstraction with OH $X_{radical}/X_{parent}$ [%]
1-naphthyl	1.17	16.00	58.58
2-naphthyl	1.48	14.50	53.39
1-acenaphthyl	0.181	0.57	2.22
3-acenaphthyl	0.076	3.06	11.67
4-acenaphthyl	0.734	2.09	7.66
5-acenaphthyl	0.152	1.78	6.56
1-pyrenyl	1.32	3.40	12.49
2-pyrenyl	1.12	2.02	7.46
4-pyrenyl	1.81	4.02	14.75

reaction (10) phenyl + C_4H_2 ⇆ 2-naphthyl at 1800 K. Peak mole fractions of phenyl and 1-naphthyl were taken from this work while a diacetylene mole fraction of 5.64 10^{-3} determined by MBMS at 0.86 cm from the burner surface [42] was used. An experimental 2-naphthyl to phenyl ratio of 0.0211 was observed compared to 0.0052 based at partial equilibrium. The compared to equilibrium conditions higher relative 2-naphthyl concentration, indicated a possible 2-naphthyl consumption via the reverse of reaction (10) and could be at least partially responsible for the small naphthyl to naphthalene ratios, shown in Table III.

Five-membered ring containing PAH have been found to isomerize easily [105,106] and the extent of equilibration between fluoranthene, acephenanthrylene and aceanthrylene have been checked in the present work. The experimental mole fraction ratios between these three compounds at 0.80 cm from the burner were found to be ≈ 10:5:1. Equilibrium conditions at 1800 K using the thermodynamic property data recently determined by Yu et al. [119] based on B3LYP/6-31G(d) density functional calculations were found to be equivalent to $X_{fluoranthene}$: $X_{acephenanthrylene}$: $X_{aceanthrylene}$ 9.4 : 5.8 : 1, i.e., equilibration between these three isomers is achieved in the limits of the uncertainties of experimental species concentrations and temperatures.

Conclusions

Radical scavenging with dimethyl disulfide after nozzle beam sampling was confirmed to be a valuable technique for the measurement of mole fraction profiles of radicals in laminar premixed low pressure flames. Thiomethyl scavenging products (R-SCH_3) were analyzed quantitatively by gas-chromatography coupled to mass spectrometry (GC-MS). Authentic standards in most cases were either available commercially or were synthesized in the present work. Sampling and trapping efficiencies were assessed and used for the determination of mole fraction profiles. Radical isomers could be distinguished and individual mole fraction profiles for phenyl, 1-,2-naphthyl, 1-,3-,4-5-acenaphthyl and 1-,2-,4-pyrenyl were measured. In addition to radicals, stable compounds up to benzo[ghi]perylene ($C_{22}H_{12}$) were collected quantitatively and identified unambiguously by means of GC-MS.

Scattering of the experimental data due to performance characteristics inherent to the equipment and to random errors was investigated. For this purpose, a nearly sooting premixed flat benzene/oxygen/argon flame (ϕ= 1.8, 30% argon, cold gas velocity v= 50 cm s^{-1}, 20 torr) was studied in two different experimental setups, one used previously in MBMS studies at MIT and one developed and built by Homann and coworkers. Mole fraction profile shape and location of all measured compounds were very similar between the two experiments while peak mole fractions were mostly lower in the experiments with the equipment from Homann and coworkers. The results of the comparison ranged from a nearly perfect match for some compounds such as for indene to ≈ 2 – 5-fold discrepancies for some other species. In a few cases such as 5-ethynylacenaphthylene, larger discrepancies were observed and attributed to possible experimental errors, particularly, incomplete peak separation in the GC analysis. These mole fraction profiles are not given in the tabulated form of the data, also available electronically. This assessment of experimental uncertainty is thought to be essential for kinetic modeling work because the experimental uncertainty sets the limits for model predictions.

A slightly sooting benzene-oxygen flame (ϕ= 2.0, 30% argon, cold gas velocity v= 50 cm s^{-1}, 20 torr) was investigated in order to assess the impact of increasing equivalence ratio on PAH formation and consumption. A shift of ≈ 2mm towards the postflame zone was observed for all PAH profiles relative to their position in the ϕ= 1.8 benzene-oxygen flame. No increase of peak

mole fractions was observed for one- and two-ring aromatics while an at least 2-fold increase was found for larger PAH. This observation might indicate a correlation between these larger PAH and the onset of soot formation.

Thermodynamic considerations were confirmed to play an important role in PAH growth. Hydrogen abstraction from PAH by H radicals rather than by OH was found to be limiting. As a general trend, partial equilibrium of (8) PAH + H ⇆ PAH• + H_2 is approached more and more closely with increasing size of the molecule. The experimental 2-naphthyl : phenyl mole fraction ratio was found to exceed the partial equilibrium value. Therefore, decomposition of PAH radicals forming butadiyne, such as by the reverse of reaction (10) phenyl + C_4H_2 ⇆ 2-naphthyl, was suggested to contribute to the consumption of some PAH radicals. Fluoranthene, acephenanthrylene and aceanthrylene, expected to interconvert easily due to the presence of a five-membered ring, were found to have at 0.80 cm from the burner, i.e., close to their maxima, mole fraction ratios of ≈ 10:5:1. Confirming easy isomerization, concentration ratios at 1800 K between these three species were calculated to be 9.4 : 5.8 : 1.

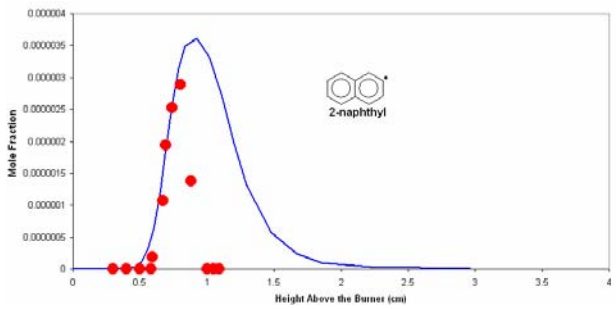

Fig. 12 Experimental and computed 2-naphthyl profiles in the nearly sooting laminar premixed benzene/oxygen/argon flame (ϕ= 1.8, 30% argon, cold gas velocity v= 50 cm s^{-1}, 20 torr).

Thermodynamic considerations are important but not sufficient for a complete understanding of PAH formation and consumption. The absence of connecting pathways on the potential energy surface or high activation energies can be prohibitive for conversions which are favorable from a thermodynamic point of view. The use of detailed kinetic models assisted by the detailed exploration of potential energy surfaces of key reactions followed by the determination of kinetic data suitable for the temperature and pressure ranges of interest is thought to be a valuable tool for deeper insight in PAH growth and consumption. The experimental data provided in this work, particularly mole fraction profiles of individual PAH radicals, are expected to help the modeling communities in these efforts.

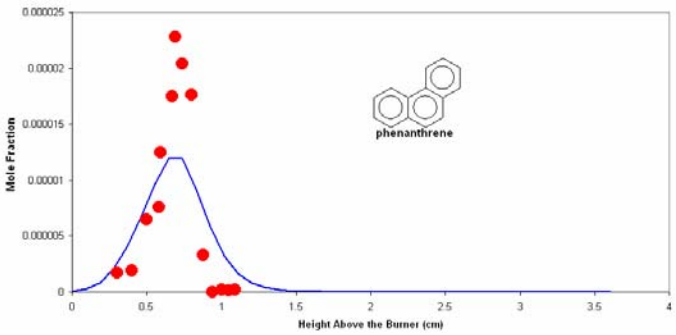

Fig. 13 Experimental and computed phenanthrene profiles in the nearly sooting laminar premixed benzene/oxygen/argon flame (ϕ= 1.8, 30% argon, cold gas velocity v= 50 cm s^{-1}, 20 torr).

B) Kinetic Modeling

The predictive capability of a detailed kinetic model was assessed by means of the newly available experimental data. The kinetic model describing PAH formation up to $C_{30}H_{10}$ has been developed over the last decade, partially with the support of the present project. Encouraging agreements between computed species concentration profiles and experimental flame structures were obtained in several benzene, acetylene, ethylene and methane flames. Major reaction pathways involved in PAH formation and depletion [120-123] have been identified and the dependence on the type of fuel has been assessed. In parallel, in NSF-funded work [124], the model was extended to carbonaceous particles with diameters of up to ≈70 nm using a discrete sectional technique [125]. In the same NSF-sponsored work, a consistent set of thermodynamic property data covering all pertinent PAH and their different radicals has been generated using B3LYP/6-31G(d) density functional calculations followed by vibrational analysis. Homodesmic reactions allowed for the determination of heats of formation [119]. The resulting detailed kinetic mechanism including PAH and soot formation, and using state-of-the-art thermodynamic property data, has been tested by comparison of its predictions with experimental data obtained in the present work. Experimental and computed 2-naphthyl concentration profiles in the laminar premixed benzene/ oxygen/argon flame (ϕ= 1.8, 30% argon, cold gas velocity v= 50 cm s^{-1}, 20 torr) flame are shown in Fig. 12 where corresponding phenanthrene profiles are given in Fig. 13. Concentration profiles of larger PAH and particles (Fig. 14) confirm the character of this flame as nearly sooting.

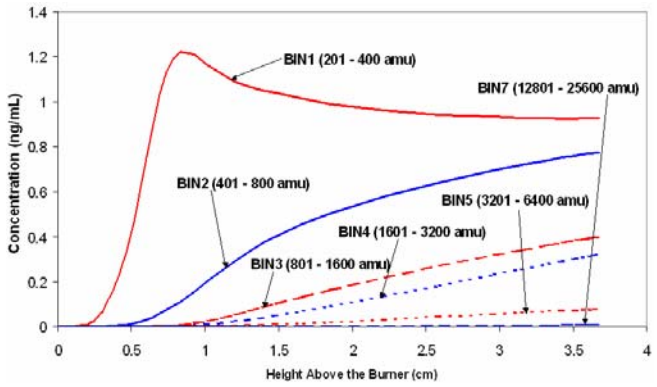

Fig. 14 Nearly sooting laminar premixed benzene/oxygen/ argon flame (ϕ= 1.8, 30% argon, cold gas velocity v= 50 cm s^{-1}, 20 torr). Large PAH and soot particles.

C) Formation of Carbon Nanotubes

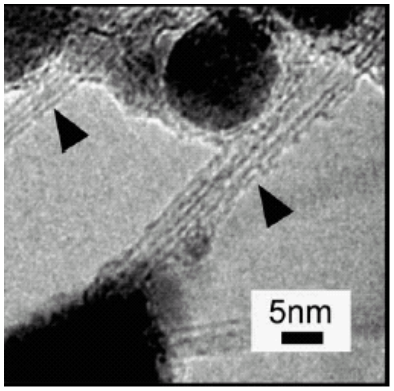

Fig. 15 High-resolution transmission electron microscopy of bundles of single-walled carbon nanotubes [126].

In studying the relationship between fullerenes formation and soot formation, it can be found that the formation of fullerenic single-walled nanotubes can be competitive with soot formation if a catalyst is present in the gas phase. In the present work, iron pentacarbonyl ($Fe(CO)_5$) was used a catalyst precursor. Liquid at standard conditions, gaseous $Fe(CO)_5$ was added to the fresh gas mixture by means of an inert carrier gas before reaching the combustion chamber. Iron-based active catalyst particles such as Fe_2O_3 are formed *in situ* in the flame. After decomposition of the $Fe(CO)_5$, oxidation and growth to particles of a suitable size, formation of single-walled carbon nanotubes is initiated. Collected material was characterized by means of Raman spectroscopy and high-resolution transmission electron microscopy (HRTEM). Details of this work have

been published [126,127]. An example of a HRTEM image showing bundles of single-walled carbon nanotubes is given in Fig. 15 [126].

References

1. Haynes, B. S. and Wagner, H. Gg., Prog. Energy Combust. Sci. 7:229-273 (1981).
2. Richter, H. and Howard, J. B., Prog. Energy Combust. Sci. 26:565-608 (2000).
3. Dockery, D. W., Pope, C. A., Xu, X., Spengler, J. D., Ware, J. H., Fay, M. E., Ferris, B. G. and Speizer, F. E., N. Engl. J. Med. 329:1753-1759 (1993).
4. Künzli, N., Kaiser, R., Medina, S., Studnicka, M., Chanel, O., Filliger, P., Herry, M., Horak Jr., F., Puybonnieux-Texier, V., Quénel, P., Schneider, J., Seethaler, R., Vergnaud, J.-C. and Sommer, H., Lancet 356:795-801 (2000).
5. Pope, C. A., Burnett, R. T. Thun, M. J., Calle, E. E., Krewski, D., Ito, K. and Thurston, G. D., JAMA 287:1132-1141 (2002).
6. Allen, J. O., Dookeran, N. M., Smith, K. A., Sarofim, A. F., Taghizadeh, K., and Lafleur, A. L., Environ. Sci. Technol. 30:1023-1031 (1996).
7. Durant, J. L., Busby, W. F., Lafleur, A. L., Penman, B. W. and Crespi, C. L., Mutation Research 371:123-157 (1996).
8. Donnet, J.-B., Bansal, R. C. and Wang, M.-J. Carbon Black : Science and Technology. 2nd edition, Dekker, New York (1993).
9. Howard, J. B., McKinnon, J, T., Makarovsky, Y. and Lafleur, A. L. and Johnson, M. E., Nature 352:139-141 (1991).
10. Howard, J. B., McKinnon, J, T., Johnson, M. E., Makarovsy, Y. and Lafleur, A. L., J. Phys. Chem. 96:6657-6662 (1992).
11. Howard, J. B., Proc. Combust. Inst. 24: 933-946 (1992).
12. Howard, J. B., Lafleur, A. L., Makarovsky, Y., Mitra, S., Pope, C. J. and Yadav, T. K., Carbon 30:1183-1201 (1992).
13. Richter, H., Fonseca, A., Emberson, S. C., Gilles, J.-M., B.Nagy, J., Thiry, P. A., Caudano, R. and Lucas, A. A., J. Chim. Phys. 92:1272-1285 (1995).
14. Richter, H., Labrocca, A. J., Grieco, W. J., Taghizadeh, K., Lafleur, A. L. and Howard, J. B., J. Phys. Chem. B 101:1556-1560 (1997).
15. Howard, J. B., Chowdhury, K. D. and Vander Sande, J. B., Nature 370:603 (1994).
16. Chowdhury, K. D., Howard, J. B. and Vander Sande, J. B., J. Mater. Res. 11:341-347 (1996).
17. Richter, H., Hernadi, K., Caudano, R., Fonseca, A., Migeon, H.-N., B.Nagy, J., Schneider, S., Vandooren, J. and Van Tiggelen, P. J., Carbon 34:427-429 (1996).
18. Grieco, W. J., Howard, J. B., Rainey, L. C. and Vander Sande, J. B., Carbon 38:597-614 (2000).
19. Vander Wal, R. L., and Ticich, T. M., Chem. Phys. Lett. 336:24-32 (2001).
20. Yuan, L., Saito, K., Hu, W., and Chen, Z., Chem. Phys. Lett. 346:23-28 (2001).
21. Lam, F. W., Howard, J. B. and Longwell, J. P., Proc. Combust. Inst. 22: 323-332 (1988).
22. Bermudez, G. and Pfefferle, L., Combust. Flame 100:41-51 (1995).
23. Chai, Y. and Pfefferle, L. D., Fuel 77:313-320 (1998).
24. Dagaut, P., PCCP

25. Marr, J. A., Giovane, L. M., Longwell, J. P., Howard, J. B., Combust. Sci. and Tech. 101:301-309 (1994).
26. Macadam, S., Beér, J. M., Sarofim, A. F. and Hoffmann, A. B., Proc. Combust. Inst. 26:2295-2302 (1996).
27. Senkan, S. and Castaldi, M., Combust. Flame 107:141-150 (1996).
28. D'Alessio, A., Gambi, G., Minutolo, P., Russo, S. and D'Anna, A., Proc. Combust. Inst. 25:645-651 (1994).
29. Marinov, N. M., Pitz, W. J., Westbrook, C. K., Castaldi, M. J. and Senkan, S. M., Modeling of Aromatic and Polycyclic Aromatic Hydrocarbon Formation in Premixed Methane and Ethane Flames. Combust. Sci. and Tech. 116-117: 211-287 (1996).
30. Crittenden, B. D. and Long, R., Combust. Flame 20:359-368 (1973).
31. Benish, T. G., Lafleur, A. L., Taghizadeh, K. and Howard, J. B., Proc. Combust. Inst. 26: 2319-2326 (1996).
32. Ciajolo, A., D'Anna, A., Barbella, R., Tregrossi, A. and Violi, A., Proc. Combust. Inst. 26: 2327-2333 (1996).
33. Castaldi, M. J., Marinov, N. M., Melius, C. F., Huang, J., Senkan, S. M., Pitz, W. J. and Westbrook, C. K., Experimental and Modeling Investigation of Aromatic and Polycyclic Aromatic Hydrocarbon Formation in a Premixed Ethylene Flame. Proc. Combust. Inst. 26: 693-702 (1996).
34. D'Anna, A. and Violi, A., Proc. Combust. Inst. 27:425-433 (1998).
35. Homann, K.-H. and Wagner, H. Gg., Proc. Combust. Inst. 11: 371-379 (1967).
36. Lamprecht, A., Atakan, B. and Kohse-Höinghaus, K., Combust. Flame 122:483-491 (2000).
37. Bockhorn, H., Fetting, F. and Wenz, H. W., Ber. Bunsenges. Phys. Chem. 87:1067-1073 (1983).
38. Kohse-Höinghaus, K., Atakan, B., Lamprecht, A., González Alatorre, G., Kamphus, M., Kasper, T. and Liu, N.-N., Phys. Chem. Chem. Phys. 4:2056-2062 (2002).
39. Atakan, B., Hartlieb, A. T., Brand, J. and Kohse-Höinghaus, K., Proc. Combust. Inst. 27:435-444 (1998).
40. Cole, J. A., Bittner, J. D., Longwell, J. P. and Howard, J. B., Combust. Flame 56:51-70 (1984).
41. Lamprecht, A., Atakan, B. and Kohse-Höinghaus, K., Proc. Combust. Inst. 28:1817-1824 (2000).
42. Bittner, J. D. and Howard, J. B., Proc. Combust. Inst. 18:1105-1116 (1981).
43. Hausmann, M., Hebgen, P. and Homann, K.-H., Proc. Combust. Inst. 24:793-801 (1992).
44. McKinnon, J. T. and Howard, J. B., Proc. Combust. Inst. 24:965-971 (1992).
45. Bachmann, M., Wiese, W. and Homann, K.-H., Proc. Combust. Inst. 26:2259-2267 (1996).
46. McKinnon, J. T., Meyer, E. and Howard, J. B., Combust. Flame 105:161-166 (1996).
47. Grieco, W. J., Lafleur, A. L., Swallow, K. C., Richter, H., Taghizadeh, K. and Howard, J. B., Proc. Combust. Inst. 27:1669-1675 (1998).
48. Tregrossi, A., Ciajolo, A. and Barbella, R., Combust. Flame 117:553-561 (1999).
49. Keller, A., Kovacs, R. and Homann, K.-H., Phys. Chem. Chem. Phys. 2:1667-1675 (2000).
50. Griesheimer, J. and Homann, K.-H., Proc. Combust. Inst. 27:1753-1759 (1998).

51. Graham, S. C., Homer, J. B., and Rosenfeld, J. L. J., Proc. R. Soc. Lond. A. 344:259-285 (1975).
52. Frenklach, M., Taki, S., Durgaprasad, M. B., and Matula, R. A., Combust. Flame 54: 81-101 (1983).
53. Frenklach, M., Ramachandra, M. K., and Matula, R. A., Proc. Combust. Inst. 20:871-878 (1984).
54. Colket, M. B., and Seery, D. J., Proc. Combust. Inst. 25:883-891 (1994).
55. Knorre, V. G., Tanke, D., Thienel, T., and Wagner, H. Gg., Proc. Combust. Inst. 26:2303-2310 (1996).
56. Böhm, H, Jander, H., and Tanke, D., Proc. Combust. Inst. 27:1605-1612 (1998).
57. Douce, F., Djebaïli-Chaumeix, N., Paillard, C.-E., Clinard, C. and Rouzaud, J.-N., Proc. Combust. Inst. 28:2523-2529 (2000).
58. Frenklach, M. and Warnatz, J., Combust. Sci. and Tech. 51:265-283 (1987).
59. Bastin, E., Delfau, J.-L., Reuillon, M., Vovelle, C and Warnatz, J, Proc. Combust. Inst. 22:313-322 (1988).
60. Wang, H. and Frenklach, M., Combust. Flame 110:173-221 (1997).
61. Richter, H., Grieco, W. J. and Howard, J. B., Combust. Flame 119:1-22 (1999).
62. Richter, H., Benish, T. G., Mazyar, O. A., Green, W. H. and Howard, J. B., Proc. Combust. Inst. 28:2609-2618 (2000).
63. Frenklach, M. and Wang, H., Detailed Mechanism and Modeling of Soot Particle Formation. In: *Soot Formation in Combustion, Mechanism and Models* (Ed., Bockhorn, H.), Springer Verlag Berlin, Springer Series in Chemical Physics 59:165-190 (1994).
64. Appel, J., Bockhorn, H. and Frenklach, M., Combust. Flame 121:122-136 (2000).
65. Mauss, F. and Bockhorn, H., Z. Phys. Chem. 188:45-60 (1995).
66. Brown, N. J., Revzan, K. L. and Frenklach, M., Proc. Combust. Inst. 27:1573-1580 (1998).
67. Hu, D., Braun-Unkhoff, M. and Frank, P., Z. Phys. Chem. 214:473-491 (2000).
68. Frenklach, M., Phys. Chem. Chem. Phys. 4:2028-2037 (2002).
69. Richter, H., Granata, S., Green, W. H. and Howard, J. B., Proc. Combust. Inst. 30:1397-1405 (2005).
70. Kunioshi, N., Touda, M. and Fukutani, S., Combust. Flame 128:292-300 (2002).
71. Kazakov, A. and Frenklach, M. Combust. Flame 112:270-274 (1998).
72. Kronholm, D. F. and Howard, J. B., Proc. Combust. Inst. 28:2555-2561 (2000).
73. Homann, K.-H., Angew. Chem., Int. Ed. Engl. 37:2434-2451 (1998).
74. Krestinin, A. V., Proc. Combust. Inst. 27:1557-1563 (1998).
75. Schottler, M. and Homann, K.-H., Ber. Bunsenges. Phys. Chem. 91:688-701 (1987).
76. Hausmann, M. and Homann, K.-H., Ber. Bunsenges. Phys. Chem. 94:1308-1312 (1990).
77. Hausmann, M. and Homann, K.-H., Ber. Bunsenges. Phys. Chem. 101:651-667 (1997).
78. Westmoreland, P. R., Howard, J. B. and Longwell, J. B., Proc. Combust. Inst. **21**, 773-782 (1986).
79. Benish, T. G., PAH Radical Scavenging in Fuel-Rich Premixed Benzene Flames. Ph.D. thesis, Massachusetts Institute of Technology, Cambridge, MA 1999.
80. McKinnon, J. T., Ph.D., Chemical and Physical Mechanisms of Soot Formation. Ph.D.

thesis, Massachusetts Institute of Technology, Cambridge, MA 1989.
81. Howard, J. B. and Bittner, J. D., Structure of Sooting Flames. In: *Soot in Combustion Systems and Its Toxic Properties.* (Ed., Lahaye, J. and Prado, G.), Plenum Press, New York and London, NATO Conference Series, VI, Materials Science 7:57-93 (1983).
82. Lindstedt, R. P. and Skevis, G., Combust. Flame 99:551-561 (1994).
83. Zhang, H.-Y. and McKinnon, J. T., Combust. Sci. and Tech. 107:261-300 (1995).
84. Tan, F. and Frank, P., Proc. Combust. Inst. 26: 677-684 (1996).
85. Richter, H. and Howard, J. B., Phys. Chem. Chem. Phys. 4:2038–2055 (2002).
86. Bachmann, M., Wiese, W. and Homann, K.-H., Combust. Flame 101:548-550 (1995).
87. Lafleur, A. L., Taghizadeh, K., Howard, J. B., Anacleto, J. F., Quilliam, M. A., J. Am. Soc. Mass Spectrom. 7:276-286 (1996).
88. Lafleur, A. L., Howard, J. B., Marr, J. A. and Yadav, T., J. Phys. Chem. 97:13539-13543 (1993).
89. Lafleur, A. L., Howard, J. B., Taghizadeh, K., Plummer, E. F., Scott, L. T., Necula, A. and Swallow, K. C., J. Phys. Chem. 100:17421-17428 (1996).
90. Scott, L. T., Bratcher, M. S. and Hagen, S., J. Am. Chem. Soc. 118:8743-8744 (1996).
91. Scott, L. T., Cheng, P.-C., Hashemi, M. M., Bratcher, M. S., Meyer, D. T. and Warren, H. B., J. Am. Chem. Soc. 119:10963-10968 (1997).
92. Scott, L. T. and Necula, A., Tetrahedron Lett. 38:1877-1880 (1997).
93. Hausmann, M. and Homann, K.-H., Ber. Bunsenges. Phys. Chem. 99:853-862 (1995).
94. Green, F. D., Remers, W. A. and Wilson, J. W., J. Am. Chem. Soc. 79:1416-1419 (1957).
95. Rasheed, K., Tetrahedron 22:2957-2966 (1966).
96. Baciocchi, E., Ruzziconi, R. and Sebastiani, G. V., J. Org. Chem. 47:3237-3241 (1982).
97. Mitchell, R. H., Chaudhary, M., Williams, R. V., Fyles, R., Gibson, J., Ashood-Smith, M. J. and Fry, A. J., Can. J. Chem. 70:1015-1021 (1992).
98. Petrenko, G. P., Tel'nyuk, E. N., Usachenko, V. C., Yampol'skya, E. Y., J. Org. Chem. USSR 4:1233-1236 (1968).
99. Lipshutz, B. H. and Hagen, W., Tetrahedron Lett. 33:5865-5868 (1992).
100. Cava, M. P., Merkel, K. E. and Schlessinger, R. H., Tetrahedron 21:3059-3064 (1965).
101. Pope, C. J. and Miller, J. A., Proc. Combust. Inst. 28:1519-1527 (2000).
102. Frenklach, M., Clary, D. W. and Gardiner, W. C. and Stein, S. E ., Proc. Combust. Inst. 21:1067-1076 (1986).
103. Richter, H., Mazyar, O. A., Sumathy, R., Green, W. H., Howard, J. B. and Bozzelli, J. W., J. Phys. Chem. A 105:1561-1573 (2001).
104. Cioslowski, J., Liu, G., Martinov, M., Piskorz, P. and Moncrieff, D., J. Am. Chem. Soc. 118:5261-5264 (1996).
105. Howard, J. B., Longwell, J. P., Marr, J. A., Pope, C. J., Busby, W. F., Lafleur, A. L. and Taghizadeh, K., Combust. Flame 101:262-270 (1995).
106. Scott, L. T. and Roelofs, N. H., J. Am. Chem. Soc. 109:5461-5465 (1987).
107. Pope. C. J., Marr, J. A. and Howard, J. B., J. Phys. Chem. 97:11001-11013 (1993).
108. Wornat, M. J., Sarofim, A. F. and Lafleur, A. L., Proc. Combust. Inst. 24:955-963 (1992).
109. Mukherjee, J., Sarofim, A. F. and Longwell, J. P., Combust. Flame 96:191-200

(1994).
110. Siegmann, K., Hepp, H. and Sattler, K., Combust. Sci. and Tech. 109:165-181 (1995).
111. Allen, J. A., Dookeran, N. M., Taghizadeh, K., Lafleur, A. L., Smith, K. A. and Sarofim, A. F., Environ. Sci. Technol. 31:2064-2070 (1997).
112. Wang, J., Ferreiro, G., Richter, H., Howard, J. B., Levendis, Y. A., and Carlson, J., Proc. Combust. Inst. 29: 2477-2484 (2002).
113. Pope, C. J. and Howard, J. B., Tetrahedron 52:5161-5178 (1996).
114. Alberty, R. A., J. Phys. Chem. 93:3299-3304 (1989).
115. Alberty, R. A., Proc. Combust. Inst. 23:487-494 (1990).
116. Kee, R. J., Rupley, F. M. and Miller, J. A. The Chemkin Thermodynamic Data Base, Sandia Technical Report SAND87-8215B, UC-4, Sandia National Laboratories, Livermore, CA, April 1994.
117. Mallard, W. G., Linstrom, P. J., Eds.: NIST Chemistry WebBook, NIST Standard Reference Database Number 69, February 2000, National Institute of Standards and Technology, Gaithersburg, MD 20899 (http://webbook.nist.gov).
118. Scott, L. T., Pure Appl. Chem. 68:291-300 (1996).
119. Yu, J., Sumathi, R. and Green, W. H., J. Am. Chem. Soc. 126:12685-12700 (2004).
120. Richter, H., Grieco, W. J. and Howard, J. B., Combust. Flame 119:1-22 (1999).
121. Richter, H., Benish, T. G., Mazyar, O. A., Green, W. H. and Howard, J. B., Proc. Combust. Inst. 28: 2609-2618 (2000).
122. Richter, H. and Howard, J. B., Phys. Chem. Chem. Phys. 4:2038-2055 (2002).
123. Dupont, L., El Bakali, A., Pauwels, J.-F., Da Costa, I., Meunier, P. and Richter, H., Combust. Flame 135:171-183 (2003).
124. National Science Foundation, Formation of Polycyclic Aromatic Hydrocarbon Structures and their Role in Soot Formation. Award 0123345, 2002.
125. Richter, H., Granata, S., Green, W. H. and Howard, J. B., Proc. Combust. Inst. 30:1397-1405 (2005).
126. Height, M. J., Howard, J. B., Tester, J. W. and Vander Sande, J. B., Carbon 42:2295-2307 (2004).
127. Height, M. J., Howard, J. B., Tester, J. W. and Vander Sande, J. B., Proc. Combust. Inst. 30:2537-2543 (2005).

Publications from Project

1. Shandross, R.A. and Howard, J.B.: "Modifications to Falloff," *QCPE Bulletin*, **7**, 73-75 and 90-91, 1987.

2. Garo, A., Westmoreland, P.R., Howard, J.B., and Longwell, J.P.: "Analysis of Fuel-Lean Combustion Using Chemical Mechanisms," *Combust. Flame*, **72**, 271-286, 1988.

3. McKinnon, J.T. and Howard, J.B.: "Critical Testing of Soot Nucleation Mechanisms," *Nineteenth Biennial Conference on Carbon*, The American Carbon Society, 390-391, 1989.

4. McKinnon, J.T., and Howard, J.B.: "Application of Soot Formation Model: Effects of Chlorine," *Combustion Science and Technology*, **74**, 175-197, 1990.

5. Howard, J.B., McKinnon, J.T., Makarovsky, Y., Lafleur, A.L., and Johnson, M.E.: "Fullerenes C_{60} and C_{70} in Flames," *Nature*, **352**, 139-141, 1991.

6. Pope, C.J. and Howard, J.B.: "Fluxes and Net Reaction Rates of Flame Species Pertinent to Fullerenes," *A.C.S. Fuel Chem. Div. Preprints*, **36 (4)**, 1541-1546, 1991.

7. Howard, J.B.: "Radical Sites as Active Sites in Carbon Addition and Oxidation Reactions at High Temperatures," *Fundamental Issues in Control of Carbon Gasification Reactivity*, J. Lahaye and P. Ehrburger, Eds., 377-382, Kluwer Academic Publishers, 1991.

8. Howard, J.B.: "Carbon Addition and Oxidation Reactions in Heterogeneous Combustion and Soot Formation *Proc. Combust. Inst.*, **23**, 1107-1127, 1991.

9. Shandross, R.A., Longwell, J.P. and Howard, J.B.: "Noncatalytic Thermocouple Coating for Low-Pressure Flames," *Combust. Flame*, **85**, 282-284, 1991.

10. Howard, J.B., McKinnon, J.T., Makarovsky, Y., Lafleur, A.L., and Johnson, M.E.: "Production and Characterization of Fullerenes in Flames," *A.C.S. Fuel Chem. Div. Preprints*, **36 (3)**, 1022-1025, 1991.

11. Anacleto, J.F., Perreault, H., Boyd, R.K., Pleasance S., Quilliam, M.A., Sim, P.G., Howard, J.B., Makarovsky, Y., and Lafleur, A.L.: "C_{60} and C_{70} Fullerene Isomers Generated in Flames. Detection and Verification by Liquid/Mass Spectrometry Analyses," *Rapid Communications in Mass Spectrometry*, **6**, 214-220, 1992.

12. Howard, J.B., McKinnon, J.T., Johnson, M.E., Makarovsky, Y. and Lafleur, A.L.: "Production of C_{60} and C_{70} Fullerenes in Benzene-Oxygen Flames," *J. Phys. Chem.*, **96**, 6657-6662, 1992.

13. Howard, J.B., Lafleur, A.L., Makarovsky, Y., Mitra, S., Pope, C.J., and Yadav, T.: "Fullerenes Synthesis in Combustion," *Carbon*, **30**, 1183-1201, 1992.

14. Mitra, S., Pope, C.J., Gleason, K.K., Makarovsky, Y., Lafleur, A.L., and Howard, J.B.: "Synthesis of Fullerenes (C_{60} and C_{70}) by Combustion of Hydrocarbons in a Flat Flame Burner," *Materials Research Society Symposium Proceedings*, **270**, 149-154, 1992.

15. Anacleto, J.F., Boyd, R.K., Pleasance, S., Quilliam, M.A., Howard, J.B., Lafleur, A.L., and Makarovsky, Y.: "Analysis of Minor Constituents in Fullerene Soots by LC-MS using a Heated Pneumatic Nebuliser. Interface with Atmospheric Pressure Chemical Ionization," *Canad. J. Chem.*, **70**, 2558-2568, 1992.

16. McKinnon, J.T. and Howard, J.B.: "The Roles of PAH and Acetylene in Soot Nucleation and Growth," *Proc. Combust. Inst.*, **24**, 965-971, 1992.

17. Howard, J.B.: "Fullerenes Formation in Flames," *Proc. Combust. Inst.*, **24**, 933-946, 1992.

18. Rotello, V.M., Howard, J.B., Yadav, T., Conn, M.M., Viani, E., Giovane, L.M., and Lafleur, A.L.: "Isolation of Fullerene Products from Flames: Structure and Synthesis of the C_{60}-Cyclopentadiene Adduct," *Tetrahedron Letters*, **34**, 1561-1562, 1993.

19. Anacleto, J.F., Quilliam, M.A., Boyd, R.K., Howard, J.B., Lafleur, A.L., and Yadav, T.: "Charge-Transfer Ionspray LC-MS Analyses of Fullerenes and Related Compounds from Flame-Generated Materials," *Rapid Communications in Mass Spectrometry*, **7**, 229-234, 1993.

20. Giovane, L.M., Barco, J.W., Yadav, T., Lafleur, A.L., Marr, J.A., Howard, J.B., Rotello, V.M.: "Kinetic Stability of the C_{60}-Cyclopentadiene Diels-Alder Adduct," *J. Phys. Chem.* **97**, 8560-8561, 1993.

21. Pope, C.J., Marr, J.A., and Howard, J.B.: "Chemistry of Fullerenes C_{60} and C_{70} Formation in Flames," *J. Phys. Chem.*, **97**, 11001-11013, 1993.

22. Lafleur, A.L., Howard, J.B., Marr, J.A., and Yadav, T.: "Proposed Fullerene Precursor Corannulene Identified in Flames Both in the Presence and Absence of Fullerenes Production," *J. Phys. Chem.*, **97**, 13539-13543, 1993.

23. Howard, J.B., Chowdhury, D.K., and Vander Sande, J.B.: "Carbon Shells in Flames," *Nature*, **370**, 603, 1994.

24. Pope, C.J., and Howard, J.B.: "Further Testing of the Fullerene Formation Mechanism with Predictions of Temperature and Pressure Effects," *Proc. Combust. Inst.*, **25**, 671-678, 1994.

25. Pope, C.J. and Howard, J.B.: "Thermochemical Properties of Curved PAH and Fullerenes: A Group Additivity Method Compared with MM3(92) and MOPAC Predictions," *J. Phys. Chem.*, **99**, 4306-4316, 1995.

26. Das Chowdhury, K., Howard, J.B., and Vander Sande, J.B.: "Fullerenic Nanostructures in Flames," *J. Materials Research*, **11**, 341-347, 1996.

27. McKinnon, J.T., Meyer, E., and Howard, J.B.: "Infrared Analysis of Flame-Generated PAH Samples," *Combust. Flame*, **105,** 161-166, 1996.

28. Lafleur, A.L. Taghizadeh, K., Howard, J.B., Anacleto, J.F., and Quilliam, M.A.: "Characterization of Flame-Generated C_{10} to C_{160} Polycyclic Aromatic Hydrocarbons by Atmospheric-Pressure Chemical Ionization Mass Spectrometry with Liquid Introduction via Nebulizer Interface," *J. Am. Soc. Mass Spectrometry*, **7,** 276-286, 1996.

29. Pope, C.J., and Howard, J.B.: "Thermodynamic Limitations for Fullerene Formation in Flames," *Tetrahedron*, **52,** 5161-5178, 1996.

30. Shandross, R.A., Longwell, J.P. and Howard, J.B.: "Destruction of Benzene in High Temperature Flames: Chemistry of Benzene and Phenol," *Proc. Combust. Inst.*, **26**, 711-719, 1996.

31. Benish, T.G., Lafleur, A.L., Taghizadeh, K., and Howard, J.B.: "C_2H_2 and PAH as Soot Growth Reactants in Premixed C_2H_4-Air Flames," *Proc. Combust. Inst.,* **26**, 2319-2325, 1996.

32. Richter, H., Taghizadeh, K., Grieco, W.J., Lafleur, A.L. and Howard, J.B.: "Preparative-Scale Liquid Chromatography and Characterization of Large Fullerenes Generated in Low Pressure Benzene Flames," *J. Phys. Chem.*, **100,** 19603-19610, 1996.

33. Lafleur, A.L., Howard, J.B., Taghizadeh, K., Plummer, E., Scott, L.T., Necula, A., and Swallow, K.C.: "Identification of $C_{20}H_{10}$ Dicyclopentapyrenes in Flames: Correlation with Corannulene and Fullerenes Formation," *J. Phys. Chem.,* **100**, 17421-17428, 1996.

34. Richter, H., Labrocca, A.J., Grieco, W.J., Taghizadeh, K., Lafleur, A L. and Howard, J.B.: "Generation of Higher Fullerenes in Flames," *J. Phys. Chem. B,* **101**, 1556-1560, 1997.

35. Lafleur, A. L., Howard, J.B., Plummer, E., Taghizadeh, K., Scott, L.C., Necula, A. and Swallow, K.C.: "Identification of Some Novel Cyclopenta-Fused Polycyclic Aromatic Hydrocarbons in Ethylene Flames," *Polycyclic Aromatic Compounds,* **12**, 223-237, 1998.

36. Shandross, R.A., Longwell, J.P. and Howard, J.B.: "Net Rate Analysis Method for Assessment and Improvement of Flame Models," *Combust. Flame*, **112**, 371-386, 1998.

37. Grieco, W.J., Lafleur, A.L., Swallow, K.C., Richter, H., Taghizadeh, K. and Howard, J.B.: "Fullerenes and PAH in Low Pressure Premixed Benzene/Oxygen Flames," *Proc. Combust. Inst.*, **27**, 1669-1675, 1998.

38. Pope, C.J., Shandross, R.A. and Howard, J.B.: "Variation of Equivalence Ratio and Element Ratios with Distance from Burner in Premixed One-Dimensional Flames," *Combust. Flame*, **116**, 605-614, 1999.

39. Richter, H., Grieco, W.J. and Howard, J.B.: "Formation Mechanism of Polycyclic Aromatic Hydrocarbons and Fullerenes in Premixed Benzene Flames," *Combust. Flame* **119**, 1-22, 1999.

40. Swallow, K.C., Howard, J.B., Grieco, W., Benish, T., Taghizadeh, K., Plummer, E.F. and Lafleur, A.L.: "Correlation of PAH Structure and Fullerenes Formation in Premixed Flames," *Polycyclic Aromatic Compounds*,**14** and **15**, 201-208(1999).

41. Richter, H. Benish, T.G., Ayala, F. and Howard, J.B.: "Kinetic Modeling of the Formation of Polycyclic Aromatic Hydrocarbons," *A.C.S. Fuel Chem. Div. Preprints* **45(2)**, 273-277, 2000.

42. Grieco, W.J., Howard, J.B., Rainey, L.C. and Vander Sande, J.B.: "Fullerenic Carbon in Combustion-Generated Soot," *Carbon* **38**, 597-614, 2000.

43. Richter, H. and Howard, J.B.: "Formation of Polycyclic Aromatic Hydrocarbons and their Growth to Soot – A Review of Chemical Reaction Pathways," *Prog. Energy and Combust. Sci.* **26**, 367-380, 2000.

44. Richter, H., Benish, T.G., Mazyar, O.A, Green, W.H. and Howard, J.B.: "Formation of Polycyclic Aromatic Hydrocarbons and Their Radicals in a Nearly Sooting Premixed Benzene Flame," *Proc. Combust. Inst.,* **28**, 2609-2618, 2001.

45. Hebgen, P., Goel, A., Howard, J.B., Rainey, L.C. and Vander Sande, J.B.: "Synthesis of Fullerenes and Fullerenic Nanostructures in a Low Pressure Benzene/Oxygen Diffusion Flame," *Proc. Combust. Inst.,* **28**, 1397-1404, 2001.

46. Richter, H., Mazyar, O.A., Green, W.H., Howard, J.B. and Bozzelli, J.W.: "A Detailed Kinetic Study of the Growth of Small Polycyclic Aromatic Hydrocarbons," *J.Phys Chem. A,* **105**, 1561-1573, 2001.

47. Goel, A., Hebgen, P., Vander Sande, J.B. and Howard, J.B.: "Combustion Synthesis of Fullerenes and Fullerenic Nanostructures," *Carbon,* **40**, 177-182, 2002.

48. Richter, H. and Howard, J.B.: "Formation and Consumption of Single-Ring Aromatic Hydrocarbons and Their Precursors in Premixed Acetylene, Ethylene and Benzene Flames", *Phy.Chem. Chem.Phys*., **4**, 2038-2055, 2002.

49. Dupont, L., El Bakali, A., Pauwels, J.-F., Da Costa, I., Meunier, P. and Richter, H.: "Investigation of Stoichiometric Methane/Air/Benzene (1.5%) and Methane/Air Low Pressure Flames", *Combust. Flame,* **135**,171-183, 2002.

50. Height, M.J., Howard, J.B., Tester, J.W.: "Flame Synthesis of Carbon Nanotubes", Materials Research Society Symposium Proceedings, **772**, 55-61 (2003).

51. Goel, A. and Howard, J.B.: "Reaction Rate Coefficient of Fullerene (C_{60}) Consumption by Soot", *Carbon*, **41**, 1949-1954, 2003.

52. Goel, A., Howard, J.B. and Vander Sande, J.B.: "Size Analysis of Single Fullerene Molecules by Electron Microscopy", *Carbon*, **42,** 1907-1915, 2004.

53. Height, M.J., Howard, J.B., Tester, J.W. and Vander Sande, J.B.: "Flame Synthesis of Single-Walled Carbon Nanotubes", *Carbon*, **42,** 2295-2307, 2004.

54. Height, M.J., Howard, J.B. and Tester, J.W.: "Flame Synthesis of Single-Walled Carbon Nanotubes", *Proc. Combust. Inst.*, **30,** 2537-2543, 2005.

55. M. Silvestrini, M., Merchan-Merchan, W., Richter, H., Saveliev, A. and Kennedy, L. A.: "Fullerenes Formation in Atmospheric Pressure Opposed Flow Oxy-Flames", *Proc. Combust. Inst.*, **30** (2004), in press.

56. Height, M.J., Howard, J.B., Tester, J. W. and Vander Sande, J.B.: "Carbon Nanotube Formation and Growth via Particle-Particle Interaction", *J. Phys. Chem. B, **109*** (in press; to appear in April, 2005 issue).